JBC Papers in Press. Published on November 22, 2005 as Manuscript M509483200
The latest version is at http://www.jbc.org/cgi/doi/10.1074/jbc.M509483200

THE CLN9 PROTEIN – A REGULATOR OF DIHYDROCERAMIDE SYNTHASE

Schulz A[1,2] , Mousallem T[1] , Venkataramani M[1] , Persaud-Sawin DA[1] , Zucker A[1], Luberto C[3] , Bielawska A[3] , Bielawski J[3] , Holthuis JCM[4] , Jazwinski SM[5] , Kozhaya L[6], Dbaibo GS[6]and Boustany R-MN[1]

Running title: CLN9, a regulator of dihydroceramide synthase

[1]Duke University Medical Center, Depts. of Pediatrics and Neurobiology, MSRB Research Drive, Box 2604, Durham, NC 27710, USA; [2]University Medical Center Hamburg, Germany, [3] MUSC, Dept. of Biochemistry, Charleston, SC, USA; [4] Utrecht University, Department of Membrane Enzymology, Utrecht, The Netherlands; [5] Louisiana State University Health Sciences Center, Dept. of Biochemistry and Molecular Biology, New Orleans, LA, USA, and [6]American University of Beirut Medical Center, Beirut, Lebanon.

Address correspondence to: Rose-Mary N. Boustany, Departments of Pediatrics and Neurobiology, MSRB Box 2604, Durham, NC 27710, USA, Tel: 919 681 6220; Fax: 919 681 8090; **E-mail: boust001@mc.duke.edu**

A new variant of a group of pediatric neurodegenerative diseases known as neuronal ceroid lipofuscinosis (NCL)§ or Batten disease has been identified. It is termed *CLN9*-deficient. *CLN9*-deficient fibroblasts have a distinctive phenotype of rapid growth and increased apoptosis, and diminished levels of ceramide, dihydroceramide and sphingomyelin. Transfection with *CLN8* but not other NCL genes, corrected growth and apoptosis in *CLN9*-deficient cells, although the entire *CLN8* sequence was normal. CLN8 is one of the TLC§ proteins containing a Lag1 motif. The latter imparts (dihydro)ceramide synthase activity to yeast cells. Transfection with the yeast gene *Lag1 Sc* and the human homolog *LASS1* increased ceramide levels, partially corrected growth and apoptosis in *CLN9*-deficient cells. *LASS2, 4, 5,* and *6* also corrected growth and apoptosis. Dihydroceramide levels and dihydroceramide synthase activity were markedly diminished in *CLN9*-deficient cells. Sequencing of *LASS1, LASS2, LASS4, LASS5,* and *LASS6* genes was normal, and expression levels were increased or normal in *CLN9*-deficient cells by RT-PCR. 4-HPR, a dihydroceramide synthase activator, corrected growth and apoptosis and increased dihydroceramide synthase activity. Ceramide levels dropped further, and there was no increase in *de novo* ceramide synthesis, probably due to the effects of 4-HPR as activator of dihydroceramide synthase and inhibitor of dihydroceramide desaturase. Fumonisin B_1, a dihydroceramide synthase inhibitor, exaggerated the *CLN9*-deficient phenotype of accelerated growth, decreased ceramide and increased apoptosis. This was neutralized by 4-HPR. We conclude that the CLN9 protein may be a regulator of dihydroceramide synthase, and that 4-HPR could be developed as a treatment for *CLN9*-deficient patients.

The neuronal ceroid lipofuscinoses (NCL) are a group of autosomal, recessively inherited storage diseases. They represent the most common cause of neurodegeneration in childhood. Neuronal death is caused by apoptosis (1). Clinical features of these diseases include visual loss, mental and motor deterioration, seizures, and early death (2-3). To date nine forms of NCL have been described. Six genes are known: *CLN1* and *CLN2* encode for the lysosomal enzymes palmitoyl protein thioesterase 1 (PPT1)§ and tripeptidylpeptidase 1 (TPP1)§, respectively (4-5). CLN5p has been described as a soluble glycoprotein (6-7). *CLN3*, *CLN6* and *CLN8* genes code for novel transmembrane proteins (8-11). Increased apoptosis has been documented in *CLN1-3, 6-* and *8*-deficient

variants (12-13).

Dysregulated sphingolipid metabolism and increased apoptosis have been described in the late infantile *CLN2*-, juvenile *CLN3*-, variant late infantile *CLN6*- and the Northern Epilepsy with Mental Retardation *CLN8*-deficient variants. CLN3 is a negative modulator of ceramide synthesis resulting in high ceramide levels in *CLN3*-deficient patient fibroblasts (14). High ceramide levels, caspase-8 activation and engagement of both the extrinsic and intrinsic apoptotic pathway, as well as caspase-dependent autophagy explain the increased apoptosis and slow growth observed in *CLN3*-deficient cells. Also, CLN3 protein harbors a galactosylceramide binding motif that is involved in CLN3 trafficking from Golgi to lipid rafts via recycling endosomes (14). The ninth form of NCL, CLN9, has recently been described in four patients, two German brothers and two Serbian sisters (15). These patients present with clinical features identical to those seen in juvenile or *CLN3*-deficient patients. The *CLN9* gene is still unknown. Mutations in all known NCL genes, including *CLN3*, were ruled out in the *CLN9*-deficient variant. *CLN9*-deficient patient fibroblasts have a distinctive phenotype. They have small and rounded cell bodies, grow rapidly, are sensitive to apoptosis and manifest a cell adhesion defect. Their gene expression pattern is significantly different from that in other NCL forms. Genes involved in cell cycle, cell adhesion and apoptosis are significantly dysregulated (www.dbsr.duke.edu/pub/cln9/). Sphingolipid metabolism, similarly to other NCL variants, is also perturbed in *CLN9*-deficient cells: Ceramide, sphingomyelin (SM)§, lactosylceramide (LacCer)§, gangliosides, ceramide trihexoside (CTH)§, and globoside (GB4)§, galactosylceramide (GalCer)§ and glucosylceramide (GluCer)§ are diminished .

The purpose of this study is to dissect out the specific biochemical defect in *CLN9*-deficient cells, with the ultimate goal of identifying the *CLN9* gene and protein. Low levels of LacCer and its metabolites including gangliosides, CTH and GB4 can implicate the seven genes for beta-1,4 galactosyltransferase (*β4GalT*)§ and the two for GB3/CD77 synthase as possible candidate genes.

Review of genechip data provided additional information: acid sphingomyelinase activity was normal, but mRNA expression of acid sphingomyelinase was 22-fold decreased in the setting of low baseline sphingomyelin levels. Defects in sphingomyelin synthase 1 and/or 2 (*SMS1*, *SMS2*)§ could account for this. A trafficking defect of ceramide from ER to Golgi due to defects in CERT§, the ER-to-Golgi ceramide transporter, could also account for low SM (16).

Low ceramide levels also suggest a defect in *de novo* ceramide synthesis. Activity of serine palmitoyltransferase (SPT), the key enzyme of *de novo* ceramide synthesis, was four-fold increased expanding the list of candidate genes to those involved in *de novo* ceramide synthesis beyond the SPT step. Transfection with *CLN8* corrected the CLN9 phenotype. The CLN8 protein contains a Lag1 motif similar to other TLC proteins (TRAM-Lag1p-CLN8) (17). Lag1p and Lac1p are homologous, multispanning transmembrane proteins that reside in the ER. Both contain a 52 amino acid long Lag1 motif that is necessary for ceramide synthesis in yeast (18-19). Lac1p, Lag1p and Lip1p are components of the enzyme activity in yeast (20). *CLN8* sequencing results were normal in *CLN9*-deficient cells, suggesting human Lag1 homologs or activators of their proteins could be candidate genes for *CLN9*.

Experimental Procedures

Cell Lines - *CLN9*-deficient fibroblast lines were derived from skin biopsies of two CLN9 patients. Use of human cell lines in research is covered by an approved Duke institutional review board protocol.

Tissue culture studies - Fibroblasts were grown at 37°C with 5% CO_2 in DMEM (Gibco-Invitrogen, Grand Island, NY, USA) containing 10% Fetal Bovine Serum (FBS) (Gibco-Invitrogen) and 1%

antibiotics/antimycotics.

Growth curves - 1 x 10^5 cells/well were plated in 6 well plates, then harvested and counted at 24, 48, 72, and 96 hours in triplicate for each time point using the Trypan blue dye exclusion method.

Trypan blue dye exclusion - Harvested cells were centrifuged at 1200 rpm for 5 min and pellets resuspended in 1:1 mixture of 4% trypan blue dye (Gibco-Invitrogen) and 1x PBS, loaded onto a hemocytometer. Viable white and dead blue cells were counted.

Etoposide treatment - Cells were treated with 10 µg/ml etoposide (Sigma, St. Louis, MO) for 18 h. Apoptosis was determined by propidium iodide (PI)§, JC-1 or TUNEL staining.

4-HPR treatment - Cells were treated with 2.5 µM, 5 µM and 10 µM 4-HPR (Sciencelab.com, Houston, TE). 4-HPR was dissolved in Ethanol at a concentration of 10 mM and stored at –20°C. Stock solutions were diluted to the required concentrations with growth medium just before use.

Fumonisin B_1 treatment - Cells were treated with 1 µM Fumonisin B_1 (FB_1)§ (Sigma, St. Louis, MO). FB_1 was dissolved in DMSO at a concentration of 1 mM and stored at -20°C. Stock solutions were diluted to the required concentration with growth medium just before use.

PDMP treatment - Cells were treated with 20 µM PDMP§ (Sigma). PDMP was dissolved in DMSO at a concentration of 20 mM and stored at -20°C. Stock solutions were diluted to the required concentration with growth medium just before use.

Transfection - Cells were transfected with different cDNA-vector constructs: *CLN1*-pGEM, *CLN2*-pGEM, *CLN3*-pGEM, *CLN6*-pGEM, *CLN8*-pGEM (cDNAs amplified and cloned as previously described), *Lag*1-pGEM, *LASS1*-pIRES2-EGFP (cDNA clones provided by S.M. Jazwinski), *LASS1trv3*-pGEM, *LASS2trv1/2*-pGEM, *LASS3*-pIRES2-EGFP, *LASS5*-pGEM (cDNA clones purchased from Open Biosystems, Huntsville, AL, USA), *LASS2trv3*-pGEM (cDNA clone purchased from OriGene Technologies Inc, Rockville, MD), *LASS4*-pBluescript (cDNA clone purchased from RZPD, Berlin, Germany). The protocols for the Lipofectamine 2000 Transfection Kit (Invitrogen-Life Technologies) were followed. The cells were washed and plated for analysis. Transfection efficiency of pGEM-transfected cells was determined using an YFP-pGEM construct and counting yellow fluorescent cells/total cells/vision field in triplicate under fluorescent microscopy. Transfection efficiency of pIRES2-EGFP-transfected cells was determined by counting green fluorescent cells/total cells/vision field in triplicate under fluorescent microscopy. Transfection efficiency of pcDNA3.1/V5-His-TOPO transfected cells was determined using a pcDNA3.1/V5-His-TOPO-LacZ construct. Transfected cells were stained using a ß-Gal Staining Kit (Invitrogen-Life Technologies). Transfection efficiency was determined counting stained cells/total cells/vision field in triplicate under light microscopy.

Sequencing - All exons including exon-intron junctions of GB3/CD77 synthase, *β4Galt1-7*, *LASS1*, *LASS2*, and *LASS4*, were amplified from genomic DNA of *CLN9*-deficient cells. Entire coding regions of *LASS5*, *LASS6*, *SMS1* and *SMS2* were amplified from cDNA of *CLN9*-deficient cells. Products were sequenced using an automated sequencer (377XL Prism DNA Sequencer; PE Biosystems, Foster City, CA, USA).

PI staining - Equal numbers of cells treated/not treated with etoposide, were grown on coverslips and stained with PI (5 µg/ml) for 5 min. Three fields of vision were chosen randomly at 100x magnification. The total number of cells/field of vision (20–60 cells/field) was counted. The number of PI-positive red apoptotic cells was determined under fluorescence (excitation wavelength: 525 nm, emission wavelength: 600 nm). The

percentage of PI-positive cells/total cells/field of vision was calculated. Average and standard deviation were determined, and statistical significance calculated using the Student's *t*-test.

JC-1 staining - JC-1§ stain (5,50-60-tetrachloro-1,1,3,3-tetraethylbenzimidazolylcarbocyanine iodide; Molecular Probes, Eugene, OR) was used to assess the decrease in mitochondrial membrane potential following treatment with etoposide. JC-1 is a cationic dye that forms J-aggregates with the cytochrome c-APAF-1 complex. Cells undergoing apoptosis are visualized when a shift in the emission spectrum from green (525 nm) to red (590 nm) occurs. This shift signals the onset of apoptosis. Equal numbers of cells treated/not treated with etoposide, were grown on coverslips. The cells were then washed with 1 x PBS and incubated with 1 mg/ml of JC-1 stain for 15 min at 37°C and in 5% CO_2. The cells were again washed in PBS and the mounted on a slide with 1:1 PBS/glycerol mix. Red apoptotic and total cells in three different fields of vision were counted (100-200 cells/field). The percentage of red apoptotic cells/total cells/field of vision was calculated, as well as average and standard deviation. Statistical significance was determined using the Student's *t*-test.

Analysis of exogenous ceramide trafficking - Equal numbers (1×10^5) of normal and *CLN9*-deficient fibroblasts were grown on coverslips and incubated in a solution containing Hank's balanced salt solution, 10mM HEPES (Gibco), 1% (w/v) fatty acid free BSA (Sigma), and 5 µm C6-NBD-ceramide at 16°C for 3 hours. Cells were then washed in Hepes-HBSS solution followed by back exchange for 30 minutes in Hepes-HBSS-BSA. Cells were mounted onto a glass slide with 1 drop of Fluoromount (Southern Biotechnology Associates, Birmingham, AL) and viewed with a Leica DMLB fluorescent microscope.

Ceramide and dihydroceramide levels - Ceramide and dihydroceramide levels were quantified by mass spectrometry (Lipidomics Core, Medical University of South Carolina) according to published methods. Ceramide and dihydroceramide levels were also measured by DGK* assay using Diacylglycerol Kinase from E. coli (Sigma) and 1.3 µCi of ATP/sample (Amersham Biosciences, Piscataway, NJ) using standards for C16, C24 and C24:1 ceramides and corresponding dihydroceramides (Avanti. Alabaster, AL).

Dihydroceramide synthase activity – Dihydroceramide synthase activity was determined by measuring *de novo* dihydroceramide generated per hour after labeling cells with C17-dihydrosphingosine (C6-dihydrosphingosine with C17 backbone) (Mol.wt.287.5 g/mole; 5 µm) for 4 hours.

Sphingomyelin synthase activity - Cells were washed three times with phosphate-buffered saline, harvested using a rubber policeman, and homogenized in 1 ml of 25 mM KCl and 25 mM Tris-Cl (pH 7.4) (TK buffer) and 0.5 mM EDTA. Cells were homogenized by 20 passages through a 27 gauge needle. Homogenates were used fresh. SM synthesis was assayed as described. The reaction mixture contained 100 µg of protein, 10 µl NBD-6-ceramide (1 mM), 1.7 µl of phosphatidylcholine (10 mg/ml), in total volume of 300 µl of TK buffer. The reaction was terminated after 90 min at 37°C by addition of 1 ml chloroform/1 ml methanol/400 µl water. Lipids were then extracted according to Bligh and Dyer and SM spots separated on TLC using chloroform/methanol/CaCl2 (15 mM) solution (120:70:16 v/v/v) as developing solvent. TLC plates were analyzed using a PhosphorImager and bands were quantified by ImageQuant software (Amersham v. 2003).

Real-time PCR - Total RNA was isolated from normal and *CLN9*-deficient fibroblasts using the Qiagen RNeasy Mini Kit (Qiagen, Valencia, CA). Reverse transcription reactions were carried out with Super Script III First-Strand-Synthesis System (Invitrogen). Real-time PCR was performed using total cDNA and Absolute QPCR SYBR Green

Fluorescence Mix (Abgene Inc., Rochester, NY) according to the manufacturer's protocol in a Biorad I-Cycler. The mRNA levels of Cyclophilin/HPRT/28S ribosomal RNA were used as internal controls.

RESULTS

CLN8 corrects growth and apoptosis in CLN9-deficient cells

CLN9-deficient fibroblasts were transfected with *CLN1, CLN2, CLN3, CLN6* and *CLN8* genes individually and were assessed for growth and sensitivity to apoptosis. Only transfection with *CLN8*, out of all NCL genes, partially corrected growth in *CLN9*-deficient cells (Fig. 1 A, B). *CLN9*-deficient cells transfected with *CLN8* cDNA showed a significant decrease in growth rate compared to *CLN9*-deficient cells transfected with empty vector. Growth rate still exceeded that of normal fibroblasts transfected with EV (Fig. 1 C). Transfection with *CLN8* decreased sensitivity to apoptosis in *CLN9*-deficient fibroblasts. Cells transfected with *CLN8* or empty vector were stained with JC-1 after 16 hours of etoposide treatment. Cells transfected with *CLN8* showed significantly less red J-aggregate formation than controls transfected with empty vector (Fig. 1 D).

Dihydroceramide synthase activity, dihydroceramide and ceramide levels are low in CLN9-deficient cells

CLN9-deficient cells have significantly decreased dihydroceramide synthase activity, as reflected by the decreased levels of dihydroceramide and ceramide in *CLN9*-deficient cells. The most significant decreases were in dhC16-, dhC24- and dhC26-ceramide and C16-, C24-, and C24:1-ceramide species compared to control cells (Fig. 2 A, B). DhC24-Cer, dhC24:1-Cer and dhC26:1-Cer levels were 4.4%, 8.2% and 9.5%, respectively, compared to normal controls.

Dihydroceramide synthase activity was measured by labeling cells with C17 dihydrosphingosine and measuring dihydroceramide generated over four hours (Fig. 5 G).

Lag1 Sc increases ceramide and corrects growth and apoptosis in CLN9-deficient cells

Transfection with *Lag1 Sc* increased total ceramide levels in *CLN9*-deficient cells 105% above levels in cells transfected with empty vector. This was determined by DGK§ assay (Fig. 3 A). Tandem mass spectrometry showed an increase in the following long chain ceramide species C18-Cer/C20-Cer/C24:1-Cer/C24-Cer*.

Lag1 Sc decreased growth rate after transfection (Fig. 3 B). *Lag1 Sc* also decreased sensitivity to apoptosis by PI staining after treatment with etoposide. Two *CLN9*-deficient cell lines had a 32.4% and 29.6% apoptotic rate after transfection with empty vector compared to a 12.8% and 4.1% apoptotic rate after transfection with *Lag1 Sc* (Fig. 3 C). Normal fibroblasts, on the other hand, had increased apoptosis after transfection with *Lag 1 Sc* (22.6% vs. 40.6%, Fig. 3 C). Baseline ceramide levels were higher in normal fibroblasts (Fig. 2 B). *Lag1 Sc* over-expression leads to higher, proapoptotic ceramide levels. In conclusion, yeast *Lag1 Sc* partially corrected ceramide levels, growth, and apoptosis in *CLN9*-deficient cells.

Human Lag1 homologs correct ceramide, growth and apoptosis in CLN9-deficient cells.

LASS1 is the human homolog to *Lag1 Sc*. *LASS1* increased total ceramide levels more than 4-fold in *CLN9*-deficient cells, as determined by DGK assay (Fig. 4 A). ^{14}C-palmitate labeling established an increase in *de novo* ceramide synthesis as well*. *LASS1* increased mass measurements of C18- and C18:1-ceramide species by 100% in normal fibroblasts and 300% in *CLN9*-deficient fibroblasts following transfection *(*Fig. 4 B). This is consistent with published reports on *LASS1* ceramide species specificity.

LASS1 partially corrected growth rate in *CLN9*-deficient cells (Fig. 4 C), and decreased cell proliferation as shown by [H3]thymidine incorporation*. *LASS1* decreased *CLN9*-deficient cell sensitivity to apoptosis as observed by PI staining (Fig. 4 D) and JC-1 staining*. *LASS1* sequences were normal in *CLN9*-deficient cells. Other human Lag1 homologs *LASS1-LASS6* (including multiple

transcript variants) were tested for their ability to correct the CLN9 phenotype. All, except *LASS3*, partially corrected growth and diminished apoptosis in *CLN9*-deficient cells*. *LASS1, LASS2, LASS4, LASS5*, and *LASS6* sequences were normal in *CLN9*-deficient cells. *LASS2* expression levels were normal, and *LASS1, 3, 4* and *6* expression levels were increased 12.7, 6.2, 9.6 and 4.3-fold excluding the possibility that the *CLN9* gene could be one of the known human Lag1 homologs.

4-HPR, increases dihydroceramide synthase activity and dihydroceramide levels, corrects growth and decreases LASS1 expression by RT-PCR

CLN9-deficient cells were treated with Fenretinide or 4-HPR, a dihydroceramide synthase activator (21). Treatment with 4-HPR increased dihydroceramide levels in both normal and *CLN9*-deficient fibroblasts. Normal fibroblasts showed an increase of all dihydroceramide species, except dhC18:1-Cer. *CLN9*-deficient cells showed an increase in all dihydroceramide species that was significantly higher than the increase in normal cells. DhC16-Cer, dhC24-Cer and dhC26:1-Cer levels increased the most after 4-HPR treatment and were elevated 244-fold, 359-fold, and 320-fold, respectively, in *CLN9*-deficient cells (Fig. 5 A). The same dihydroceramide species had the lowest levels in untreated *CLN9*-deficient cells (Fig. 2 A).

Dihydroceramide synthase activity was also increased by 4-HPR (Fig. 5 G). There was, however, no increase in rate of *de novo* ceramide synthesis after 4-HPR treatment in *CLN9*-deficient cells as measured by ^{14}C-Palmitate labeling. Treatment with 4-HPR decreased levels of all ceramide species as measured by tandem mass spectrometry (Fig. 5 B). This effect might be due to a combined action of 4-HPR as activator of dihydroceramide synthase and inhibitor of dihydroceramide desaturase #.

Treatment with 4-HPR corrected growth of *CLN9*-deficient cells in a time- and dose-dependent manner. Continuous treatment with 4-HPR at the same concentration showed significant decrease of growth in *CLN9*-deficient cells after 48 hours (Fig. 5 C). Treatment with 2.5 µM 4-HPR did not have a significant effect on growth, but 5 µM and 10 µM 4-HPR decreased growth in a dose-dependent manner (Fig. 5 C). There was no effect of 4-HPR on growth of normal cells when used at the same concentration*. 4-HPR decreased *LASS1* expression to 0.22-fold in mRNA from untreated *CLN9*-deficient cells. In normal cells 4-HPR decreased *LASS1* expression to 0.5-fold expression from normal fibroblasts.

4-HPR or PDMP protect CLN9-deficient cells from apoptosis

Treatment with 4-HPR protected *CLN9*-deficient cells from apoptosis. Cells treated with 4-HPR showed significantly less apoptosis by PI staining (20.4% untreated vs. 5.4% treated with 5 µM 4-HPR). This effect was dose-dependent. 10 µM 4-HPR decreased apoptosis even further (4.1%; Fig. 5 D). These results were confirmed by JC-1 and TUNEL staining.

4-HPR normally increases apoptosis (22). *CLN9*-deficient cells were protected from apoptosis by 4-HPR. Treating *CLN9*-deficient cells with PDMP, which inhibits glucosylceramide synthase, results in an increase in ceramide mass measurements (23). PDMP diminished apoptosis in *CLN9*-deficient cells. Treatment with PDMP and 4-HPR, however, increased apoptosis above the level of untreated *CLN9*-deficient cells. This was determined by PI staining (Fig. 5 E). This effect may be due to the combined effect of an increase in ceramide due to PDMP, and an increase in dihydroceramide due to 4-HPR (Fig. 5 F). These drugs act at different steps of the pathway.

Fumonisin B_1, a dihydroceramide synthase inhibitor, exaggerates the CLN9 phenotype

To confirm that the CLN9-phenotype could be due to a defect in activation of dihydroceramide synthase, fumonisin B_1 (FB_1) was used. It inhibits dihydroceramide synthase and should, therefore, exaggerate the CLN9-phenotype. Pretreatment with FB_1 decreased baseline low ceramide levels in *CLN9*-deficient cells even further. 4-HPR neutralized the effect of FB_1 on ceramide

levels. Ceramide levels were measured by DGK assay after 34 hours of 4-HPR treatment (Fig. 6 A). FB_1 treatment accelerated growth of *CLN9*-deficient cells exaggerating the CLN9 phenotype. Treatment with 4-HPR opposed this increase in growth (Fig. 6 B). *CLN9*-deficient cells pretreated with FB_1 also had a higher apoptotic rate than untreated cells. FB_1 opposed the protective effect of 4-HPR. The effects on apoptosis were amplified in the presence of etoposide as visualized by PI staining and confirmed by JC-1 staining (Fig. 6 C).

Low sphingomyelin in CLN9-deficient cells is not due to a ceramide trafficking defect

Ceramide produced at the endoplasmic reticulum (ER) is transported via CERT or ceramide transporter protein to the lumen of the Golgi for conversion to sphingomyelin (SM) by sphingomyelin synthase 1 (16). Should a ceramide trafficking defect be present, sphingomyelin synthase activity would be elevated. Sphingomyelin synthase activity was 40% of normal negating the possibility of a ceramide trafficking defect in *CLN9*-deficient cells. Also, *CLN9*-deficient cells when exposed to fluorescent NBD-C6-ceramide, demonstrated an intensely fluorescent Golgi reflecting normal trafficking and uptake of ceramide with conversion to SM in the Golgi lumen (Fig. 7).

The CLN9-phenotype is best explained by the extremely low dihydroceramide and ceramide levels. Increasing dihydroceramide by 4-HPR, or ceramide by PDMP corrected the phenotype.

DISCUSSION

CLN9-deficient cells manifest increased apoptosis, but accelerated growth combined with very low ceramide levels (15). The marked decrease in *de novo* LacCer synthesis and glycosphingolipids and gangliosides derived from it begged the question of whether one of the seven β-1,4 galactosyltransferases (*β4GalT 1-7*)§ or GB3/CD77 synthase could be candidates for *CLN9*. All seven β4GalT proteins are membrane proteins that reside in the Golgi, and the latter is also the seat of SM synthesis from ceramide, and LacCer synthesis from GluCer (24-25). A defect in *β4GalT7* had already been described in a patient with a progeroid, Ehlers-Danlos-like syndrome (26). We ruled out mutations in these genes in CLN9 patients by sequence analysis. Low sphingomyelin suggested a possible defect in sphingomyelin synthesis. SM synthase proteins SMS1 and SMS2 reside in the Golgi and the plasma membrane, respectively (27-28). Sphingomyelin synthase activities were 40 % of normal and sequences of both of *SMS1* and *SMS2* were intact in *CLN9*-deficient cells. Also, *SMS1* and *SMS2* gene expression in *CLN9*-deficient cells was comparable to normal. Moreover, overexpression of *SMS1* or *SMS2* in *CLN9*-deficient cells had no effect on growth, essentially ruling them out as candidate genes for *CLN9*.

Transfection with *CLN8* corrected growth and decreased apoptosis in *CLN9*-deficient cells. Human dihydroceramide synthase is still poorly characterized. Overexpression of the yeast gene *Lag1 Sc* and *LASS1*, the human Lag1 homolog for *Lag1 Sc*, complemented the defect in CLN9 cells with correction of ceramide levels, growth and apoptosis.

The inhibiting effect of ceramide on cell growth is well known. The mouse homologue of Lag1 increases C18-ceramide and decrease cell growth in HNSCC (Head and Neck Squamous Cell Carcinoma) cells derived from head and neck tumors (29). *LASS1 Hs* is primarily expressed in brain, with very low levels of expression in skeletal muscle and testis. Genes involved in neurodegenerative diseases have a distribution pattern similar to that of human *LASS1* or *LASS1 Hs* (30). Analysis of tissue distribution of mouse *LASS1, LASS2, LASS4, LASS5,* and *LASS6* confirmed that only LASS1 expression was mostly brain specific (31). A normal *LASS1* sequence, as well as elevated levels of gene expression in *CLN9*-deficient cells excludes *LASS1* from being a candidate for *CLN9*. All other human Lag1 homologs, except *LASS3*, could partially correct growth and apoptosis in *CLN9*-deficient cells. *LASS3* contains both a Lag1 motif and a Hox domain. Studies in yeast cells led to the hypothesis that both

motifs are important for ceramide synthesis (32). Our results indicate that in mammalian cells this is not necessarily true. Transfection with either *LASS1*, *LASS2* transcript variant 1 or 2, or *LASS2* transcript variant 3 corrected growth and apoptosis in *CLN9*-deficient cells. *LASS2* transcript variants 1 and 2 contain both a Lag1 motif and a Hox domain. *LASS2* transcript variant 3 lacks the Hox domain, but was still able to complement CLN9. Only the Lag1 motif, and not the Hox domain, is sufficient and necessary for ceramide synthesis in human fibroblasts. Low dihydroceramide level, and low *de novo* dihydroceramide synthesis and increases in *LASS1*, *LASS3*, *LASS4* and *LASS6* expression by RT-PCR, suggest that CLN9 may be a modulator of dihydroceramide synthase at the protein level. 4-HPR, an activator of dihydroceramide synthase, increased dihydroceramide levels in *CLN9*-deficient cells. Dihydroceramide levels were markedly increased in both *CLN9*-deficient and normal fibroblasts by the drug. 4-HPR increased *de novo* dihydroceramide synthesis, but did not increase *de novo* synthesis or mass levels of ceramide. This was not surprising as 4-HPR also inhibits dihydroceramide desaturase #.

Increases in dihydroceramide levels in *CLN9*-deficient cells corrected growth and decreased apoptosis. Dihydroceramide has been found to be biologically inactive in some cell systems (33). The data from *CLN9*-deficient cells presented here suggest that dihydroceramide may be biologically active when ceramide levels are extremely low, resulting in modulation of growth and apoptosis.

4-HPR is used as a ceramide-modulating chemotherapeutic agent. A dose and time dependent increase in ceramide after 4-HPR treatment has been described in neuroblastoma cell lines, in prostate and breast cancer cells, lymphoblastic leukemia cells and Ewing family tumors as well (34-38). Maurer et al. showed that 4-HPR did not increase ceramide in non-malignant fibroblasts and EBV-transformed lymphoblastoid cell lines (39). Our data also suggest that 4-HPR has different biologic effects depending on baseline ceramide and dihydroceramide levels of the specific cell type: there is protection from apoptosis in *CLN9*-deficient cells and an increase in apoptosis in normal fibroblasts. We hypothesize that base line dihydroceramide and ceramide levels in cells determine the effect of 4-HPR on apoptosis. Dihydroceramide levels in *CLN9*-deficient cells are increased by treatment with 4-HPR, but ceramide levels are lowered even further. PDMP increases ceramide but not dihydroceramide levels. Each of the treatments alone results in protection from apoptosis. Treatment with both 4-HPR and PDMP increased apoptosis in *CLN9*-deficient cells. This is most likely due to a simultaneous increase of dihydroceramide and ceramide levels. 4-HPR can cause both apoptosis and p53- and caspase-independent cell loss without increases in ceramide (22). Lovat et al. describe that inhibitors of acid sphingomyelinase, but not dihydroceramide synthase, block 4-HPR induced apoptosis in neuroblastoma cells (40). Treatment with both 4-HPR and Desipramine, an inhibitor of acid sphingomyelinase, did not change the protective effect of 4-HPR on apoptosis in *CLN9*-deficient fibroblasts*. There are two paradoxes here: 4-HPR protects *CLN9*-deficient cells from apoptosis, and this occurs in the setting of an increase in dihydroceramide and a further decrease in ceramide levels. PDMP, which increases ceramide levels, but has no effect on dihydroceramide levels, also protects these cells from apoptosis. This can be explained in multiple ways: 1) a threshold lower level of ceramide is necessary for the well-being of cells, below which apoptosis is activated; 2) when ceramide levels are very low, dihydroceramide assumes some of the biologic functions of ceramide, and the sum total of ceramide and dihydroceramide determines biologic function; or, 3) variations in levels of other biologically active sphingolipid metabolite(s) can explain these findings.

The findings of low dihydroceramide levels, and partial correction of the *CLN9*-deficient phenotype by human *LAG1* homologs, except *LASS3*, suggested that *CLN9* could be a human Lag1 homolog or a regulator of dihydroceramide synthase.

Normal Lag1 homolog sequences, elevated levels of expression of human *LASS* genes by RT-PCR, increases in dihydroceramide levels and a drop in *LASS1* expression in response to 4-HPR, however, indicate that *CLN9* could be an activator of dihydroceramide synthase, should the mutation in CLN9 result in loss of function. Likewise, a gain of mutation function such as in a duplication of a gene, or a CLN9 mutation resulting in tighter binding of the inhibitor to dihydroceramide synthase may suggest that CLN9 or mutated CLN9 could be an inhibitor of dihydroceramide synthase activity at the protein level. This work also has diagnostic and therapeutic implications: determination of dihydroceramide levels by tandem mass spectrometry can be developed as a diagnostic test for ascertainment of new *CLN9*-deficient cases. Moreover, the oral drug 4-HPR, a dihydroceramide synthase activator, may also have potential as a treatment option for *CLN9*-deficient patients.

Acknowledgement

This work was supported by the Deutsche Forschungsgemeinschaft (SCHU1597/1-1, A.S.) and by the Serbian Orthodox Church (R.-M.B.). We thank the affected families for participating in this study.

REFERENCES

1. Lane, S. C., Jolly, R. D., Schmechel, D. E., Alroy, J., and Boustany, R. M. (1996) *J. Neurochem.* **67**, 677-683.
2. Goebel, H. H., Mole, S. E., and Lake, B. D. (1999) *IOS Press*.
3. Haltia, M. (2003) *J. Neuropathol. Exp. Neurol.* **62**, 1-13.
4. Vesa, J., Hellsten, E., Verkruyse, L. A., Camp L. A., Santavuori, P., Hofman, S. L., and Peltonen, L. (1995) *Nature* **376**, 584-587.
5. Sleat, D. E., Donnelly, R. J., Lackland, H., Liu, C. G., Sohar, I., Pullarkat, R. K., and Lobel, P. (1997) *Science* **277**, 1802-1805.
6. Savukoski, M., Klockars, T., Holmberg, V., Santavuori, P., Lander, E. S., and Peltonen, L. (1998) *Nat. Genet*. **19**, 286-288.
7. Isosomppi, J., Vesa, J., Jalanko, A., and Peltonen, L. (2002) *Hum. Mol. Genet*. **11**, 885-891.
8. International Batten Disease Consortium. (1995) *Cell* **82**, 949-957.
9. Gao, H., Boustany, R. M., Espinola, J. A., Cotman, S. L., Srinidhi, L., Antonellis, K. A., Gillis, T., Qin, X., Liu, S., Donahue, L. R., Bronson, R. T., Faust, J. R., Stout, D., Haines, J. L., Lerner, T. J., and MacDonald M. E. (2002) *Am. J. Hum. Genet.* **70**, 324-335.
10. Wheeler, R. B., Sharp, J. D., Schultz, R. A., Joslin, J. M., Williams, R. E., and Mole, S. E. (2002) *Am. J. Hum. Genet*. **70**, 537-542.
11. Ranta, S., Zhang, Y., Ross, B., Lonka, L., Takkunen, E., Messer, A., Sharp, J., Wheeler, R., Kusumi, K., Mole, S., Liu, W., Soares, M. B., Bonaldo, M. F., Hirvasniemi, A., de la Chapelle, A., Gilliam, T. C., and Lehesjoki, A. E. (1999*) Nat. Genet*. **23,** 233-236.
12. Cho, S., Dawson, P. E., Dawson, G. (2001) *Eur. J. Paed. Neurol.* **5**, 53-55.
13. Lane, S., Jolly, R., Schmechel, D., Alroy, J., Boustany, R. M. (1996) J. Neurochemistry **67**, 677-683.
14. Persaud-Sawin, D. A., McNamara II, J. O., Rylova, S., Vandongen, A., and Boustany, R. M. (2004) *Ped. Res.* **56**, 449-463.
15. Schulz, A., Dhar, S., Rylova, S., Dbaibo, G., Alroy, J., Hagel, C., Artacho, I., Kohlschütter, A., Lin, S. and Boustany, R. M. (2004) *Ann. Neurol*. **56**, 341-350.
16. Hanada, K., Kumagai, K., Yasuda, S., Miura, Y., Kawano, M., Fukasawa, M., and Nishijima, M. (2003) *Nature* **426**, 803-809.
17. Winter, E., Ponting, C. P. (2002) *Trends Biochem. Sci*. **27**, 381-383.
18. Guillas, I., Kirchman, P. A., Chuard, R., Pfefferli, M., Jiang, J. C., Jazwinski, S. M., and Conzelmann, A. (2001) *EMBO J*. **20**, 2655-2665.
19. Schorling, S., Vallee, B., Barz, W. P., Riezmann, H., and Oesterhelt, D. (2001) *Mol. Biol. Cell* **12**, 3417-3427.
20. Vallee, B., and Riezmann, H. (2005) *EMBO J*. **24**, 730-741.

21. Wang, H., Maurer, B. J., Reynolds, C. P., and Cabot, M. C. (2001) *Cancer Res*. **61**, 5102-5105.
22. Maurer, B. J., Metelitsa, L. S., Seeger, R. C., Cabot, M. C., and Reynolds, C. P. (1999) *J. Natl. Cancer Inst.* **91**, 1138-1146.
23. Abe, A., Inokuchi, J., Jimbo, M., Shimeno, H., Nagamatsu, A., Shayman, J. A., Shukla, G. S., and Radin, N. S. (1992) *J. Biol. Chem.* **111**, 191-196.
24. Amado, M., Almeida, R., Schwientek, T., and Clausen, H. (1999) *Biochim. Phys. Acta* **1473**, 35-53.
25. Hennet, T. (2002) *Cell. Mol. Life Sci*. **59**, 1081-1095.
26. Kresse, H., Rosthoj, S., Quentin, E., Hollmann, J., Glossl, J., Okada, S., and Tonnesen, T. (1987) *Am. J. Hum. Genet.* **41**, 436-453.
27. Huitema, K., van den Dikkenberg, J., Brouwers, J. F. H. M., and Hlothuis, J. C. M. (2004) *EMBO J*. **23**, 33-44.
28. Yamaoka, S., Miyaji, M., Kitano, T., Umehara, H., and Okazaki, T. (2004) *J. Biol. Chem.* **18**, 18688-18693.
29. Koybasi, S., Senkal, C. E., Sundararaj, K., Spassieva, S., Bielawski, J., Osta, W., Day, T. A., Jiang, J. C., Jazwinski, S. M., Hannun, Y. A., Obeid, L. M., and Ogretmen, B. (2004) *J. Biol. Chem.* **279**, 44311-44319.
30. Jiang, J. C., Kirchman, P. A., Zagulski, M., Hunt, J., and Jazwinski, S. M. (1998) *Genome Res*. **8**, 1259-1272.
31. Mizutani, Y., Kihara, A., and Igarashi, Y. (2005) *Biochem. J.* **390**, 263-271.
32. Venkataraman, K., and Futerman, A. H. (2002) *FEBS Letters* **528**, 3-4.
33. Lee, J. Y., Hannun, Y. A., and Obeid, L. M. (1996) *J. Biol. Chem.* **271**, 13169-13174.
34. Garaventa, A., Luksch, R., Lo Piccolo, M. S., Cavadini, E., Montaldo, P. G., Pizzitola, M. R., Boni, L., Ponzoni, M., Decensi, A., De Bernardi, B., Fossati Bellani, F., and Formelli, F. (2003) *Clin. Cancer Res*. **9**, 2032-2039.
35. Wang, H., Charles, A. G., Frankel, A. J., and Cabot, M. C. *Urology* **61**, 1047-1052.
36. Veronesi, U., De Palo, G., Marubini, E., Costa, A., Formelli, F., Mariani, L., Decensi, A., Camerini, T., Rosselli Del Turco, M., Di Mauro, M. G., Miceli, R., and Sporn, M. B. (1999) *J. Natl. Cancer Inst.* **91**, 1847-1856.
37. Faderl, S., Lotan, R., Kantarjian, H. M., Harris, D., Van, Q., and Estrov, Z. (2003) Leuk. Res. 27, 259-266.
38. Batra, S., Reynolds, C. P., Maurer, B. J. (2004) Cancer Res. 64, 5415-5424.
39. Maurer, B. J., Melton, L., Billups, C., Cabot, M. C., and Reynolds, C. P. (2000) *J. Natl. Cancer Inst.* **92**, 1897-1909.
40. Lovat, P. E., Di Sano, F., Corazzari, M., Fazi, B., Donnorso, R. P., Pearson, A. D. J., Hall, A. G., Redfern, C. P. F., and Piacentini, M. (2004) *J. Natl. Cancer Inst.* **96**, 1288-1299.

Footnotes:* data not shown; # Alfred Merrill, personal communication, 2004

§ Abbreviations:
NCL= neuronal ceroid lipofuscinosis), **TLC**= TRAM-Lag1-CLN8, **4-HPR**=N-(4-hydroxyphenyl)retinamide, **PPT1**= palmitoyl protein thioesterase 1 **TPP1** = tripeptidylpeptidase 1, **Cer** = ceramide, **SM** = sphingomyelin, **GluCer**= glucosylceramide,**GalCer** = galactosylceramide, **LacCer** = lactosylceramide, **CTH** = ceramide trihexoside ,**GB4** = globoside ,**ß4GalT**= beta-1,4 galactosyltransferase, **GB3/CD77**= globoside synthase **SMS1/SMS2** = sphingomyelin synthase, **CERT** = ceramide transporter protein), **SPT**= serine palmitoyltransferase, **TRAM** = translocating chain-associated membrane protein , **PI** = propidium iodide, **JC-1** = 5,50-60-tetrachloro-1,1,3,3-tetraethylbenzimidazolylcarbocyanine iodide, **FB_1**= fumonisin B_1, **PDMP**= phenyl-2-decanoulamino-3-morpholino-1-propranolol), **EV**= empty vector, **DGK** = diacylglycerol kinase **TLC**= thin layer chromatography,**CS**= dihydroceramide synthase

Legends

Fig. 1. Transfection with CLN8 corrects growth and decreases apoptosis in CLN9-deficient cells. (A) Growth curve of *CLN9*-deficient fibroblasts transfected with *CLN1* (diamond), *CLN2* (square) and *CLN8* (triangle). Live cells were counted in triplicate at different timepoints. (B) Growth curve of *CLN9*-deficient fibroblasts transfected with *CLN3* (diamond), *CLN6* (square), empty vector (EV, circle) and *CLN8* (triangle). Live cells were counted in triplicate at different timepoints. A significant decrease in growth rate is seen in cells transfected with *CLN8*. (C) Growth curve of *CLN9*-deficient fibroblasts transfected with empty vector (EV, square) or *CLN8* (triangle) and normal fibroblasts transfected with empty vector (EV, diamond). A significant decrease in growth rate is seen in cells transfected with *CLN8*. Growth rate of empty vector transfected normal fibroblasts is even lower. (D) JC-1-staining of *CLN9*-deficient fibroblasts transfected with EV or *CLN8* after etoposide treatment. Apoptotic cells are red, healthy cells are green. *CLN8* decreases apoptosis (number of green healthy cells).

Fig. 2. Low dihydroceramide and ceramide levels in CLN9-deficient cells. (A) Dihydroceramide species levels are significantly decreased in *CLN9*-deficient cells compared to normal fibroblasts (NF). Dihydroceramide levels were measured by tandem mass spectrometry (values from single measures are shown). (B) Ceramide species levels in *CLN9*-deficient cells are significantly decreased in *CLN9*-deficient cells compared to normal fibroblasts (NF). Ceramide levels were measured by tandem mass spectrometry (values from single measures are shown).

Fig. 3. Lag1 Sc corrects ceramide levels and growth rate and decreases apoptosis in CLN9-deficient cells. (A) Transfection with *Lag1 Sc* increases ceramide levels compared to transfection with empty vector (EV) in *CLN9*-deficient cells (DGK-assay). (B) Growth curve of *CLN9*-deficient fibroblasts transfected with *Lag1 Sc* (triangle) or empty vector (EV, square). Live cells were counted in triplicates at different timepoints. A significant decrease in growth rate is seen in cells transfected with *Lag1 Sc*. (C) Propidium iodide staining of normal (NF) and two *CLN9*-deficient fibroblast cell lines [CLN9(1) and CLN9(2)] after treatment with etoposide. Transfection with *Lag1 Sc* increases the number of PI positive apoptotic cells in normal fibroblasts (22.6% vs. 40.6%, p-Value 0.04) and decreases the number of PI-positive apoptotic

cells in *CLN9*-deficient fibroblasts compared to empty vector transfection (32.4% / 29.6% vs. 12.8% / 4.1%, p-Values 0.006 / 0.001).

Fig. 4. LASS1 corrects ceramide levels, growth rate and decreases apoptosis in CLN9-deficient cells. (A) Transfection of *CLN9*-deficient cells with *LASS1* increases ceramide levels compared to transfection with empty vector (EV) (DGK-assay). (B) Transfection with *LASS1* increases levels of C18-Cer and C18:1-Cer species in both normal (NF) and *CLN9*-deficient fibroblasts (values from single measures by tandem mass spectrometry are shown). (C) *CLN9*-deficient fibroblasts transfected with *LASS1* (triangle) or empty vector (EV, square). Live cells were counted in triplicates at different timepoints. A significant decrease in growth rate is seen in cells transfected with *LASS1*. (D) Propidium iodide staining of two *CLN9*-deficient fibroblast cell lines [CLN9(1) and CLN9(2)] after treatment with etoposide. Transfection with *LASS1* decreases the number of PI-positive apoptotic cells in *CLN9*-deficient fibroblasts compared to empty vector transfection.

Fig.5. 4-HPR activates dihydroceramide synthase, corrects dihydroceramide levels, growth and decreases apoptosis in CLN9-deficient cells. (A) Treatment with 4-HPR increases dihydroceramide species levels more significantly in *CLN9*-deficient cells than in normal fibroblasts (NF) as measured by tandem mass spectrometry. Fold changes compared to untreated control are shown (values from single measures). (B) Treatment with 4-HPR decreases ceramide species levels in *CLN9*-deficient and normal fibroblasts (NF) as measured by tandem mass spectrometry (values from single measures). (C) Growth curve of *CLN9*-deficient fibroblasts untreated (diamond), treated with 2.5 µM 4-HPR (square), 5 µM 4-HPR (triangle), and 10 µM 4-HPR (circle). Live cells were counted in triplicates at different timepoints. A significant dose-dependent decrease in growth rate is seen in cells treated with 4-HPR. (D-E) Propidium iodide staining of *CLN9*-deficient fibroblasts after treatment with 4-HPR and/or PDMP. Treatment with 4-HPR decreases the number of PI-positive apoptotic cells in a dose-dependent manner (20.4% untreated vs. 5.4%/4.1% treated with 5 µM/10 µM 4-HPR, p-Value 0.009). Treatment with PDMP decreases the number of PI-positive apoptotic cells. Treatment with both, 4-HPR and PDMP, increases the number of PI-positive apoptotic cells. (F) DGK assay measuring ceramide and dihydroceramide in *CLN9*-deficient cells treated with 4-HPR alone, PDMP alone, or both. Note that the combined total of ceramide and dihydroceramide is very low in untreated cells, somewhat higher in 4-HPR (~2-fold) and PDMP (~1.5 fold) treated cells, but much higher in 4 HPR+PDMP treated cells (~5-fold). (G) Dihydroceramide synthase activity: d*e novo* C17 dihydroceramide generation over 4 hours before and after treatment with 4-HPR (values from single measures by tandem mass spectrometry). Treatment with 4-HPR increases *de novo* dihydroceramide generation (reflecting increased dihydroceramide synthase activity).

Fig.6. Opposing effects of 4-HPR and FB_1 on ceramide levels, growth and apoptosis. (A) Treatment with FB1 decreases ceramide and dihydroceramide levels in *CLN9*-deficient cells measured at 34 hours by DGK assay. Treatment with 4-HPR neutralizes the effect of FB_1 on ceramide and dihydroceramide levels. (B) Growth curve of *CLN9*-deficient fibroblasts untreated (diamond), pretreated with FB_1 (square), treated with 4-HPR (triangle), and treated with both, FB_1 and 4-HPR (circle). Live cells were counted in triplicate at different timepoints. FB_1 treatment increases the growth rate, exaggerating the *CLN9*-deficient phenotype. Treatment with 4-HPR neutralizes the increase in growth after FB_1. (C) Propidium iodide staining of *CLN9*-deficient fibroblasts treated with FB_1 and/or 4-HPR. Treament with FB_1 increases apoptosis in *CLN9*-deficient cells even more, and opposes the protective effect of 4-HPR on apoptosis. This is shown in cells without and with etoposide treatment.

Fig. 7. Cer traffics correctly from ER to Golgi lumen in normal and CLN9-deficient cells.
Treatment of normal (lower panel) and *CLN9*-deficient fibroblasts (upper panel) with

fluorescently labeled NBD C-6 ceramide at 16°C for 3 hours results in uptake of ceramide by the Golgi with conversion to sphingomyelin within the Golgi lumen by sphingomyelin synthase 1. White arrows point to eccentric intensely fluorescent Golgi next to an oval shaped dark nucleus. Note much smaller *CLN9*-deficient cells (magnification X 100).

Fig. 8. Schematic of the sphingolipid synthetic pathway. The sites of action of the various sphingolipid activators and inhibitors used in this study and the location of the hypothesized CLN9 action are indicated. Green arrows represent activating action, red lines represent inhibiting action.

l A

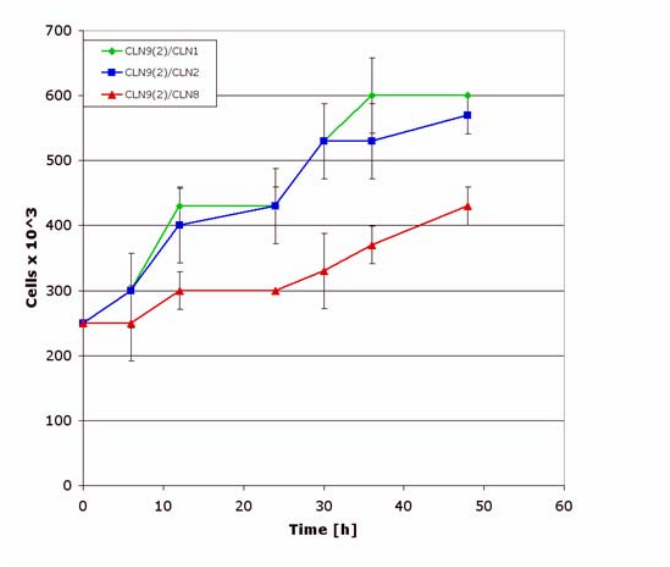
CLN9(2)/CLN1
CLN9(2)/CLN2
CLN9(2)/CLN8
Cells x 10^3
Time [h]
0
100
200
300
400
500
600
700
0
10
20
30
40
50
60

B

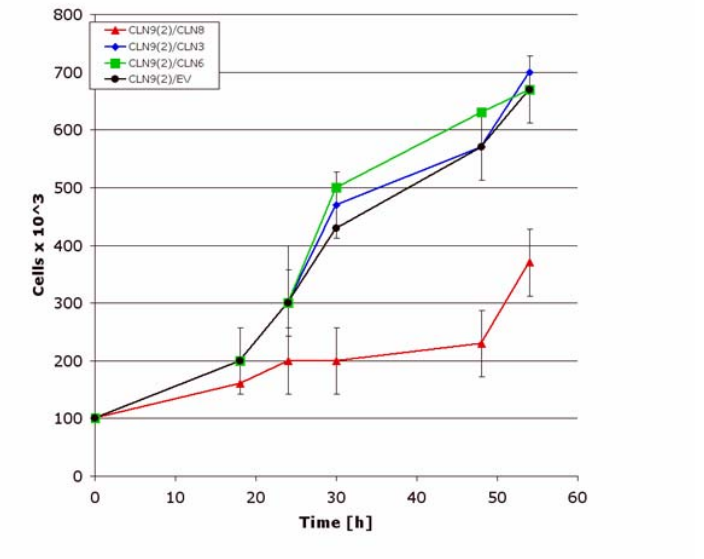
CLN9(2)/CLN8
CLN9(2)/CLN3
CLN9(2)/CLN6
CLN9(2)/EV
Cells x 10^3
Time [h]
0
100
200
300
400
500
600
700
800
0
10
20
30
40
50
60

1 C

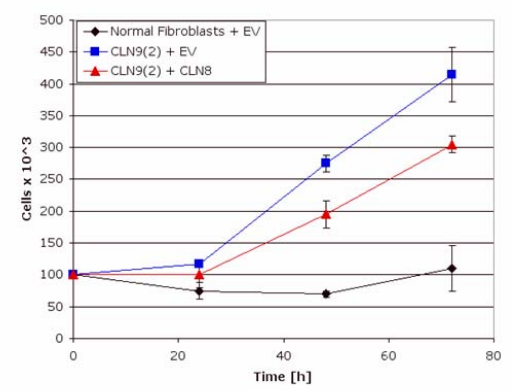
Normal Fibroblasts + EV
CLN9(2) + EV
CLN9(2) + CLN8
Cells x 10^3
Time [h]
0
50
100
150
200
250
300
350
400
450
500
0
20
40
60
80

1 D

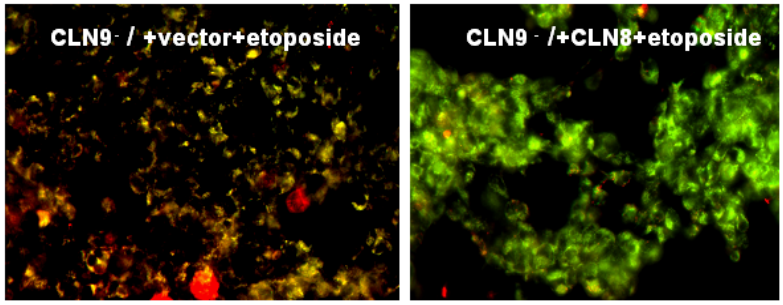
CLN9- / +vector+etoposide
CLN9 - /+CLN8+etoposide

2A

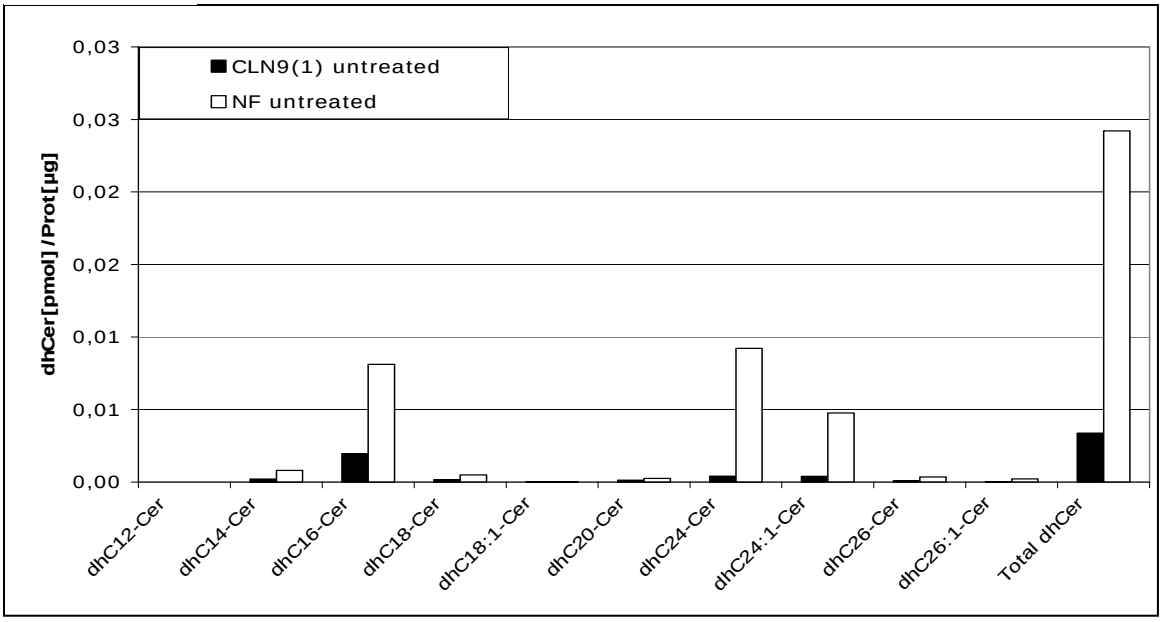
CLN9(1) untreated
NF untreated
dhCer[pmol] /Prot[µg]
0,03
0,03
0,02
0,02
0,01
0,01
0,00
dhC12-Cer
dhC14-Cer
dhC16-Cer
dhC18-Cer
dhC18:1-Cer
dhC20-Cer
dhC24-Cer
dhC24:1-Cer
dhC26-Cer
dhC26:1-Cer
Total dhCer

2B

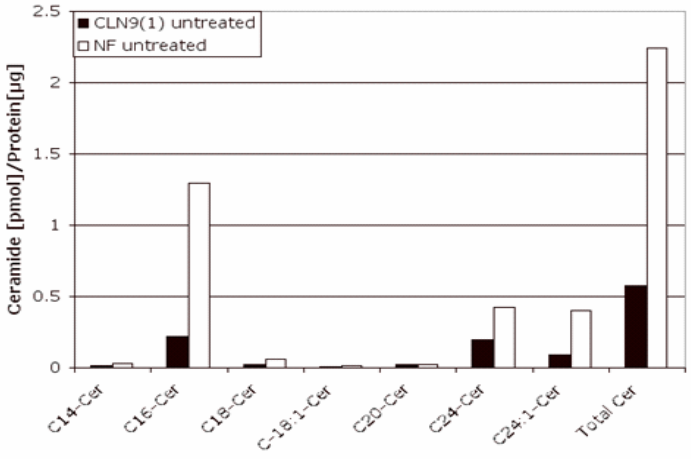
CLN9(1) untreated
NF untreated
Ceramide [pmol]/Protein[µg]
2.5
2
1.5
1
0.5
0
C14-Cer
C16-Cer
C18-Cer
C-18:1-Cer
C20-Cer
C24-Cer
C24:1-Cer
Total Cer

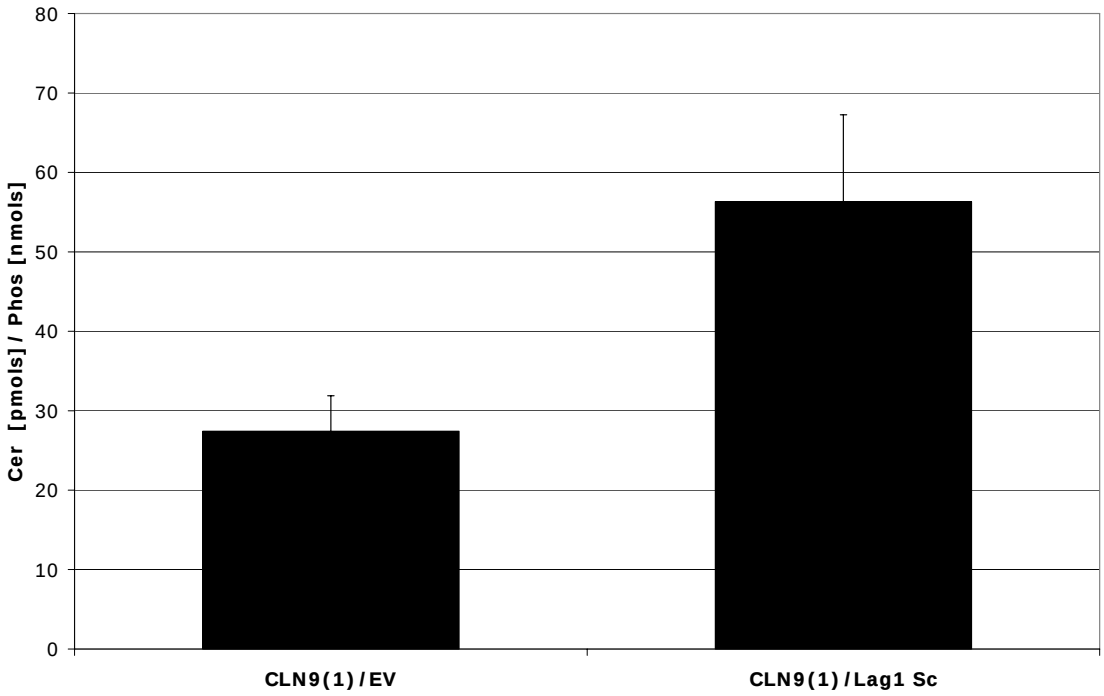
80
70
60
50
40
30
20
10
0
Cer [pmols] / Phos [nmols]
CLN9(1)/EV
CLN9(1)/Lag1 Sc

Fig. 3 A

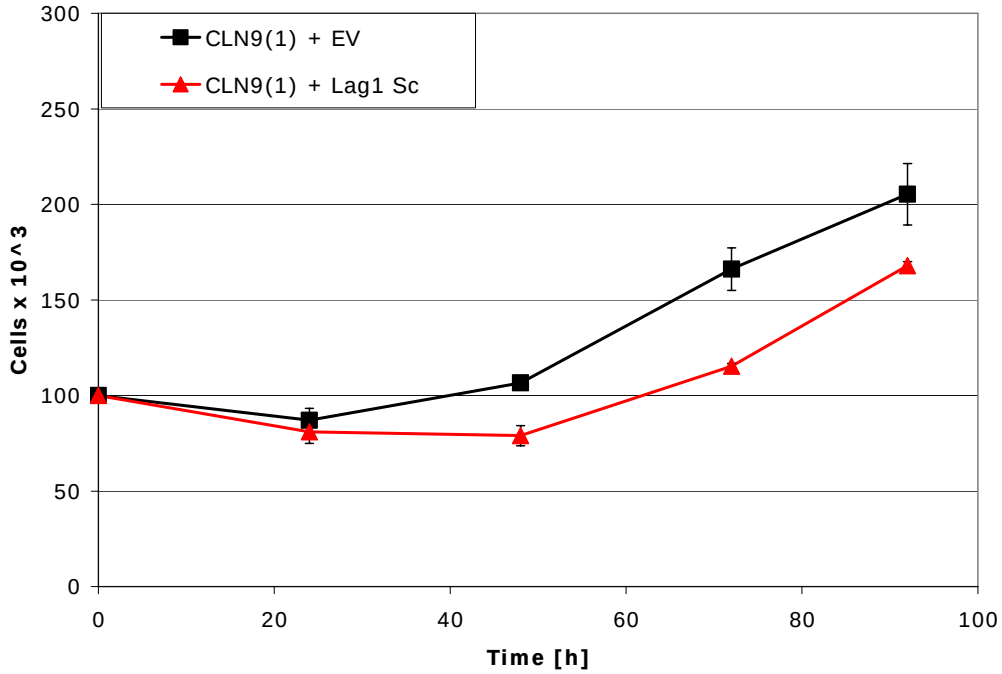
CLN9(1) + EV
CLN9(1) + Lag1 Sc
300
250
200
150
100
50
0
Cells x 10^3
0
20
40
60
80
100
Time [h]

Fig. 3 B

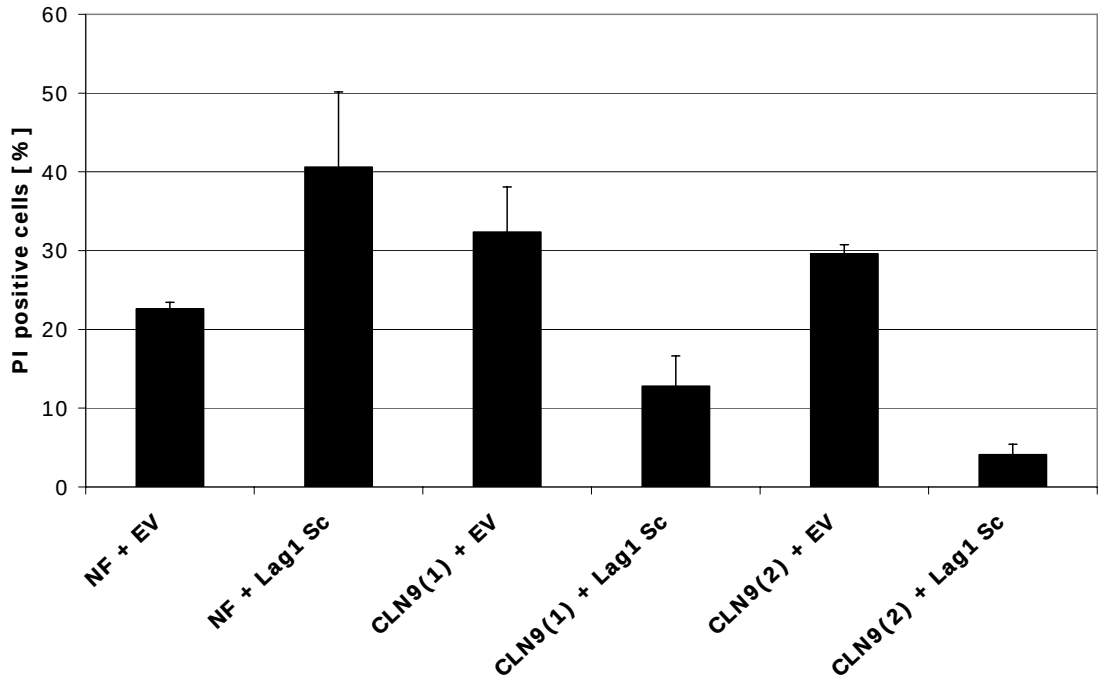
PI positive cells [%]
60
50
40
30
20
10
0
NF + EV
NF + Lag1 Sc
CLN9(1) + EV
CLN9(1) + Lag1 Sc
CLN9(2) + EV
CLN9(2) + Lag1 Sc

Fig. 3 C

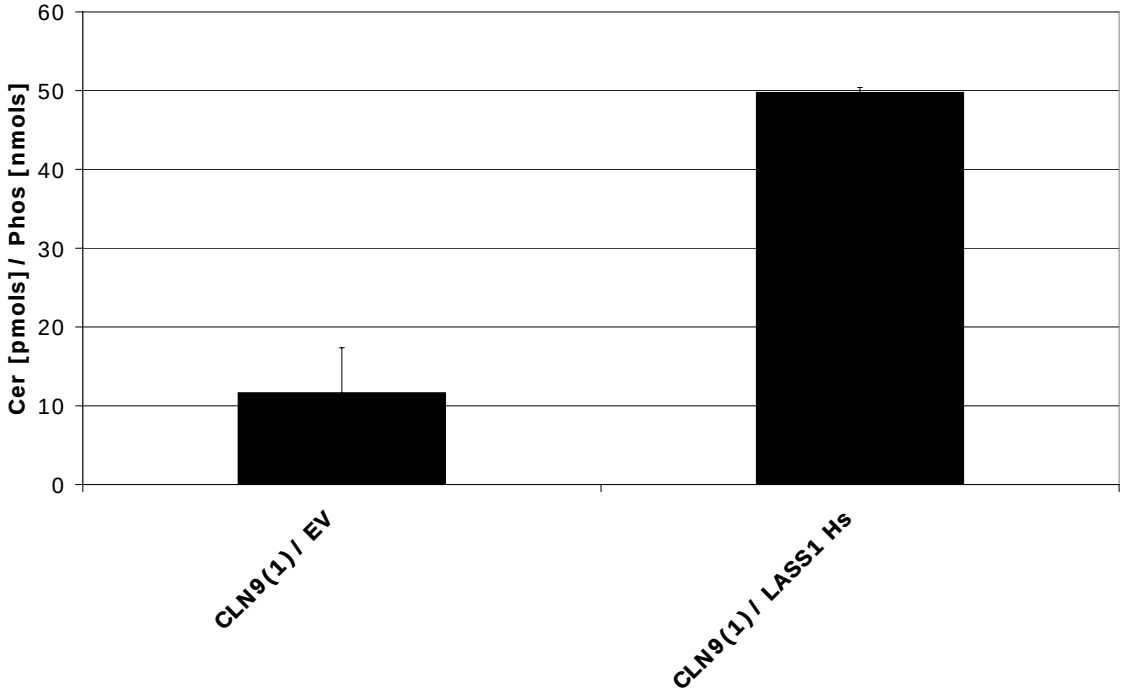
Cer [pmols] / Phos [nmols]
60
50
40
30
20
10
0
CLN9(1) / EV
CLN9(1) / LASS1 Hs

Fig. 4 A

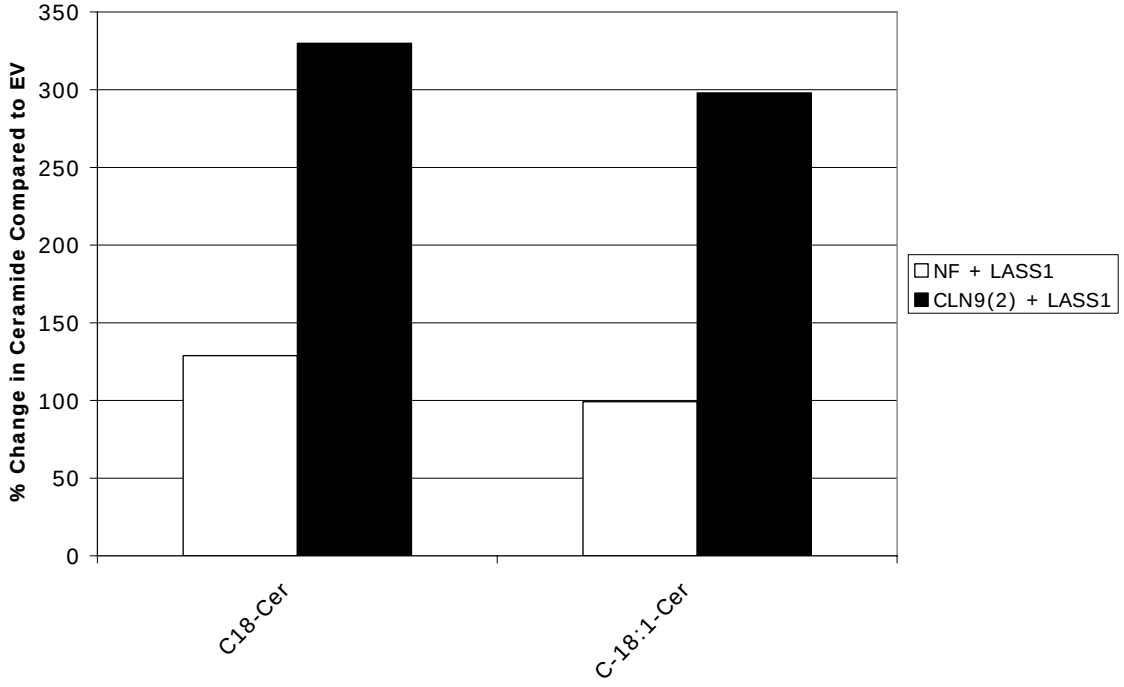
% Change in Ceramide Compared to EV
350
300
250
200
150
100
50
0
C18-Cer
C-18:1-Cer
NF + LASS1
CLN9(2) + LASS1

Fig. 4 B

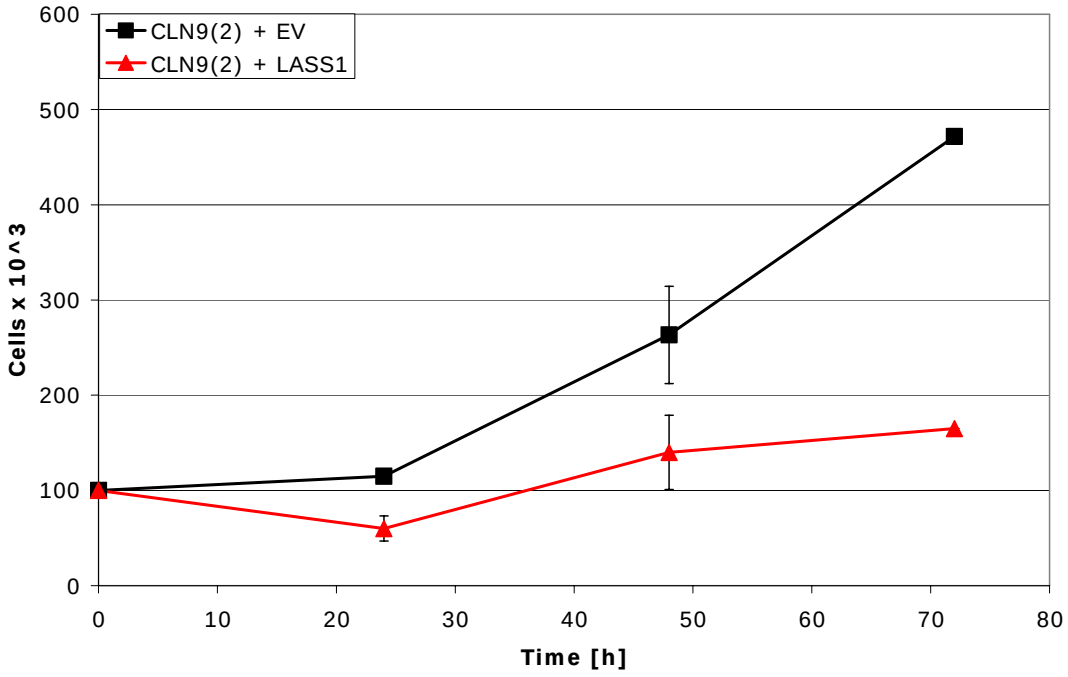
CLN9(2) + EV
CLN9(2) + LASS1
Cells x 10^3
600
500
400
300
200
100
0
0
10
20
30
40
50
60
70
80
Time [h]

Fig. 4 C

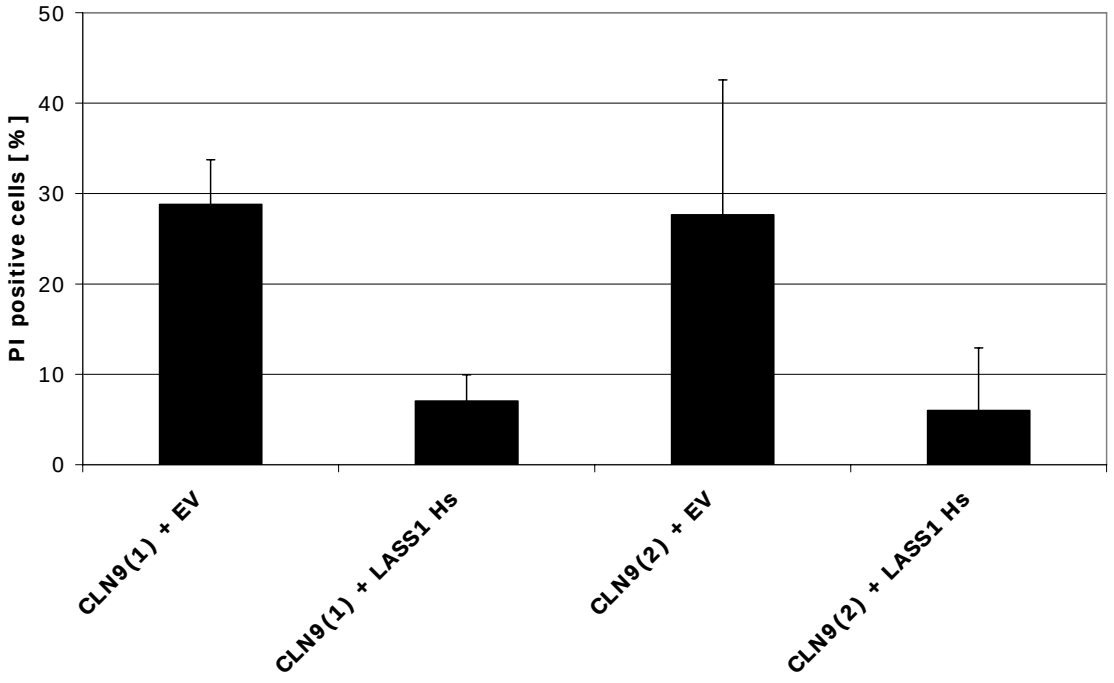
PI positive cells [%]
50
40
30
20
10
0
CLN9(1) + EV
CLN9(1) + LASS1 Hs
CLN9(2) + EV
CLN9(2) + LASS1 Hs

Fig. 4 D

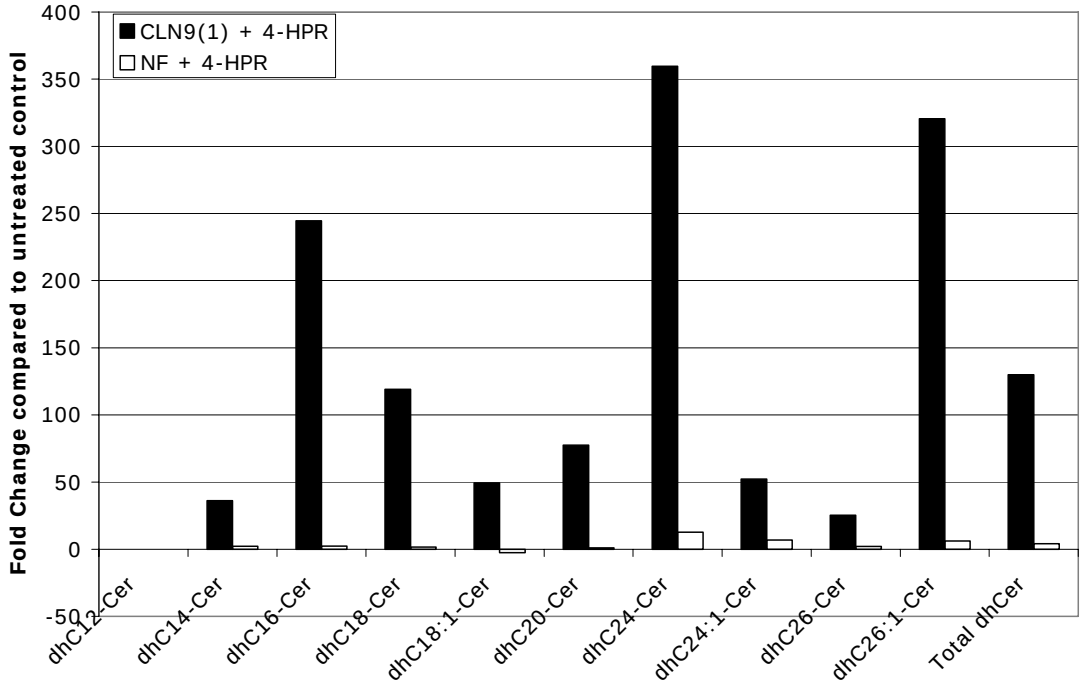
CLN9(1) + 4-HPR
NF + 4-HPR
Fold Change compared to untreated control
400
350
300
250
200
150
100
50
0
-50
dhC12-Cer
dhC14-Cer
dhC16-Cer
dhC18-Cer
dhC18:1-Cer
dhC20-Cer
dhC24-Cer
dhC24:1-Cer
dhC26-Cer
dhC26:1-Cer
Total dhCer

Fig. 5 A

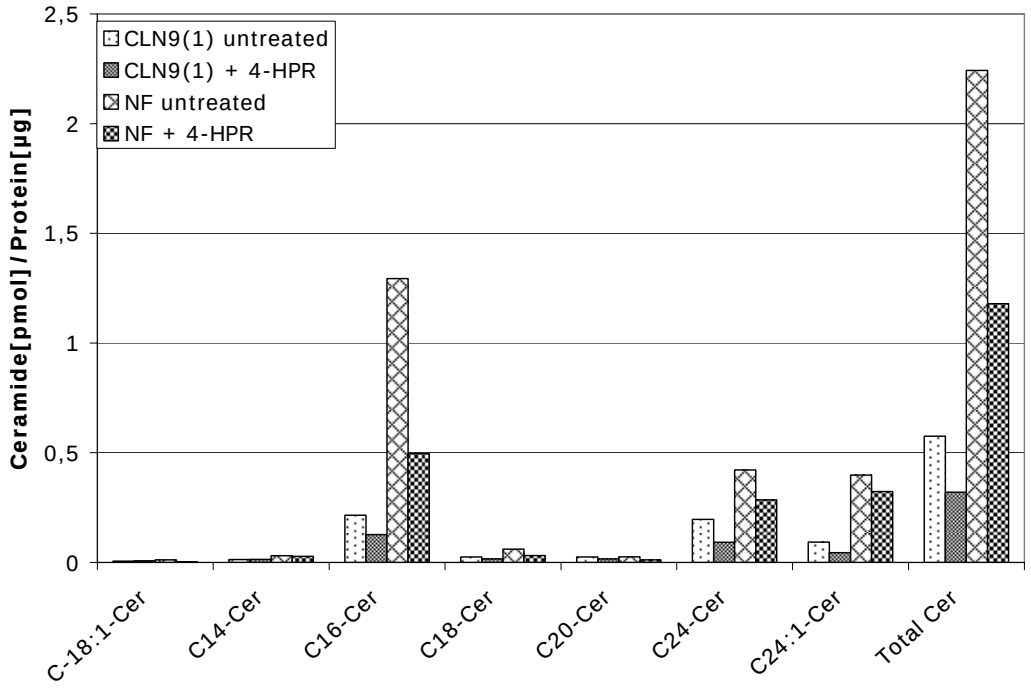
CLN9(1) untreated
CLN9(1) + 4-HPR
NF untreated
NF + 4-HPR
Ceramide[pmol]/Protein[µg]
2,5
2
1,5
1
0,5
0
C-18:1-Cer
C14-Cer
C16-Cer
C18-Cer
C20-Cer
C24-Cer
C24:1-Cer
Total Cer

Fig. 5 B

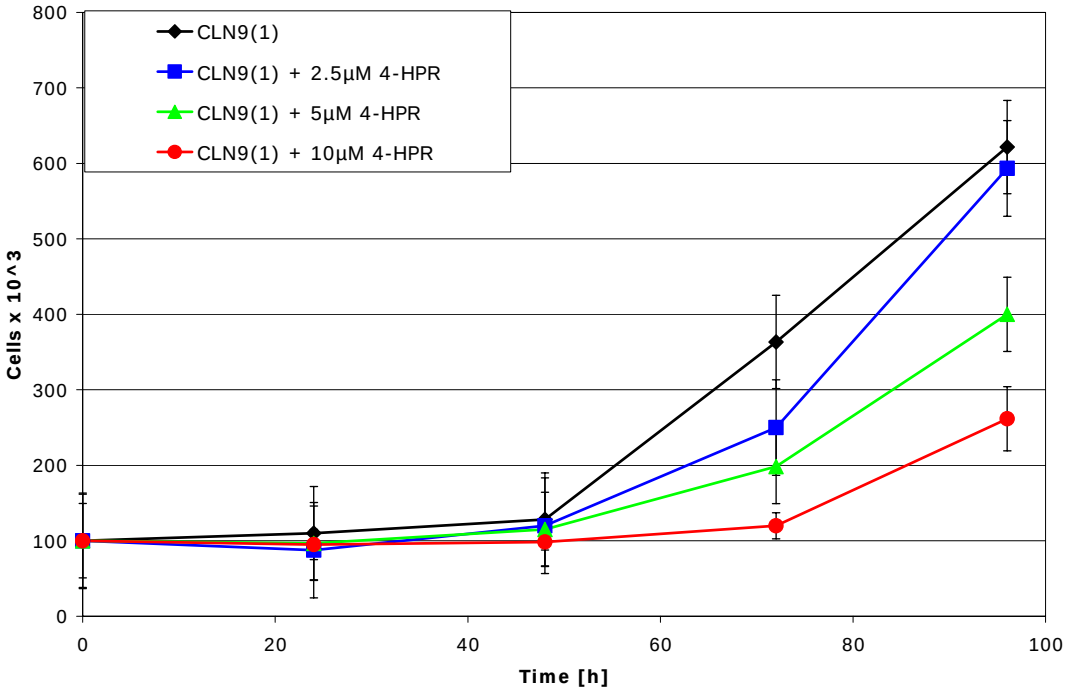
CLN9(1)
CLN9(1) + 2.5µM 4-HPR
CLN9(1) + 5µM 4-HPR
CLN9(1) + 10µM 4-HPR
Cells x 10^3
800
700
600
500
400
300
200
100
0
0
20
40
60
80
100
Time [h]

Fig. 5 C

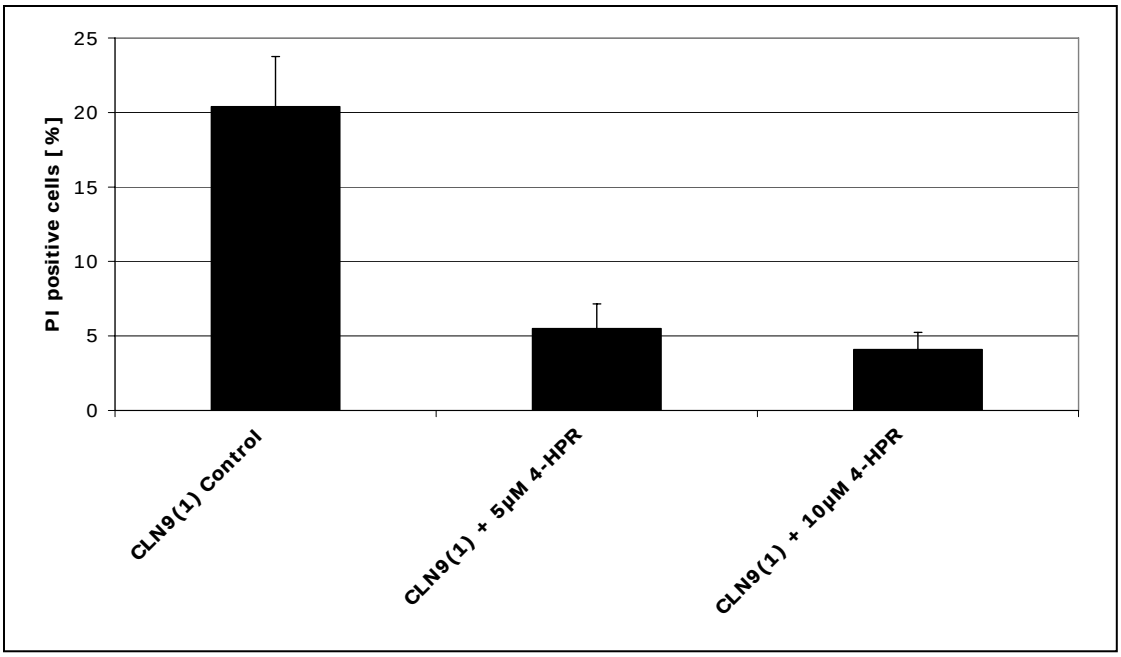
PI positive cells [%]
25
20
15
10
5
0
CLN9(1) Control
CLN9(1) + 5µM 4-HPR
CLN9(1) + 10µM 4-HPR

5D

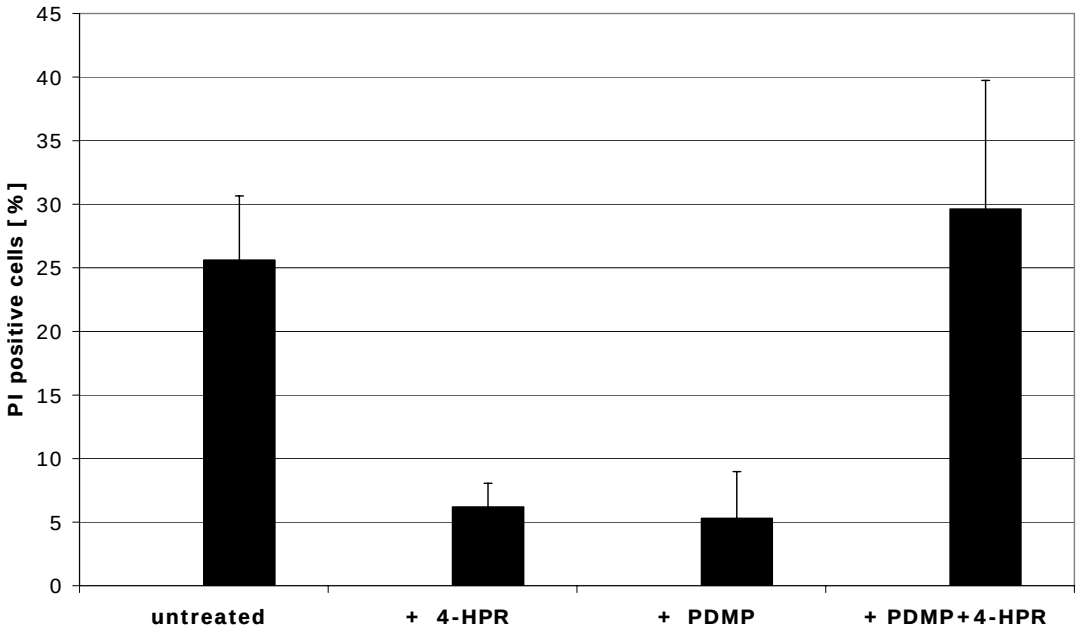
PI positive cells [%]
45
40
35
30
25
20
15
10
5
0
untreated
+ 4-HPR
+ PDMP
+ PDMP+4-HPR

5E

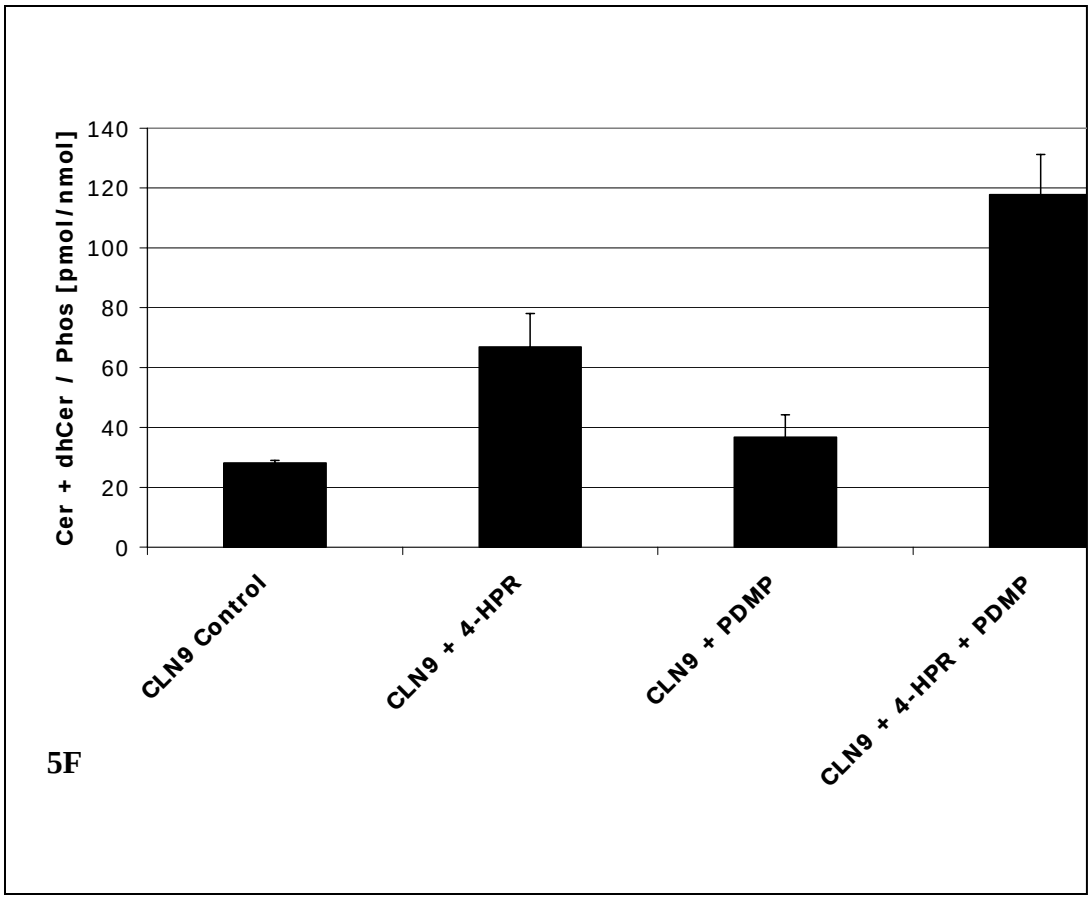
Cer + dhCer / Phos [pmol/nmol]
140
120
100
80
60
40
20
0
CLN9 Control
CLN9 + 4-HPR
CLN9 + PDMP
CLN9 + 4-HPR + PDMP

5F

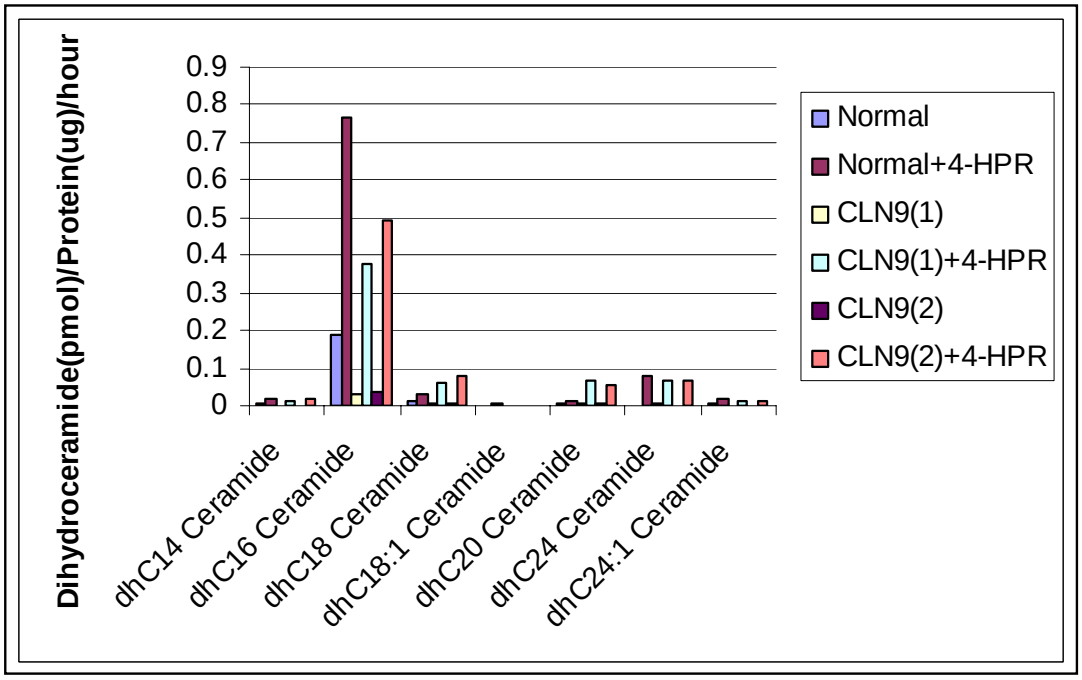
Dihydroceramide(pmol)/Protein(ug)/hour
0.9
0.8
0.7
0.6
0.5
0.4
0.3
0.2
0.1
0
dhC14 Ceramide
dhC16 Ceramide
dhC18 Ceramide
dhC18:1 Ceramide
dhC20 Ceramide
dhC24 Ceramide
dhC24:1 Ceramide
Normal
Normal+4-HPR
CLN9(1)
CLN9(1)+4-HPR
CLN9(2)
CLN9(2)+4-HPR

5G

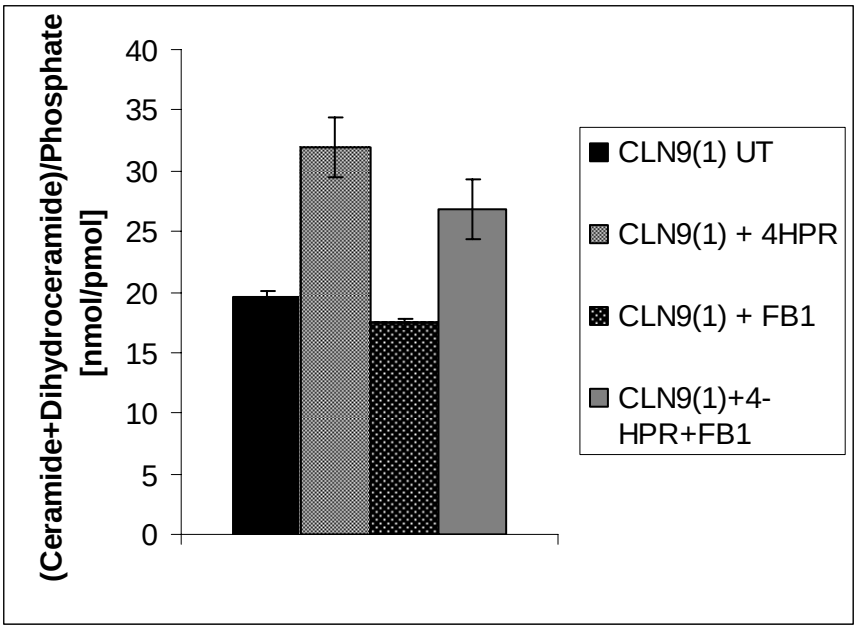
(Ceramide+Dihydroceramide)/Phosphate [nmol/pmol]
40
35
30
25
20
15
10
5
0
CLN9(1) UT
CLN9(1) + 4HPR
CLN9(1) + FB1
CLN9(1)+4-HPR+FB1

6A

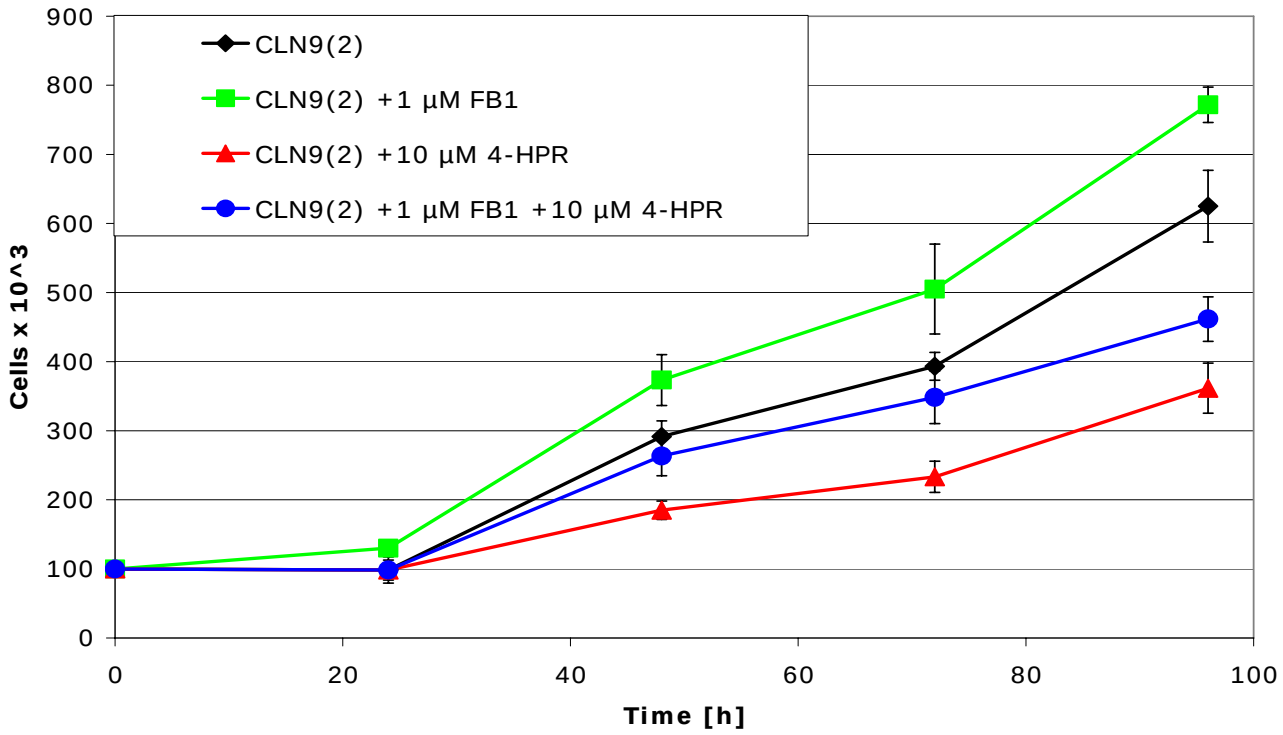
CLN9(2)
CLN9(2) +1 µM FB1
CLN9(2) +10 µM 4-HPR
CLN9(2) +1 µM FB1 +10 µM 4-HPR
Cells x 10^3
Time [h]
900
800
700
600
500
400
300
200
100
0
0
20
40
60
80
100

Fig. 6 B

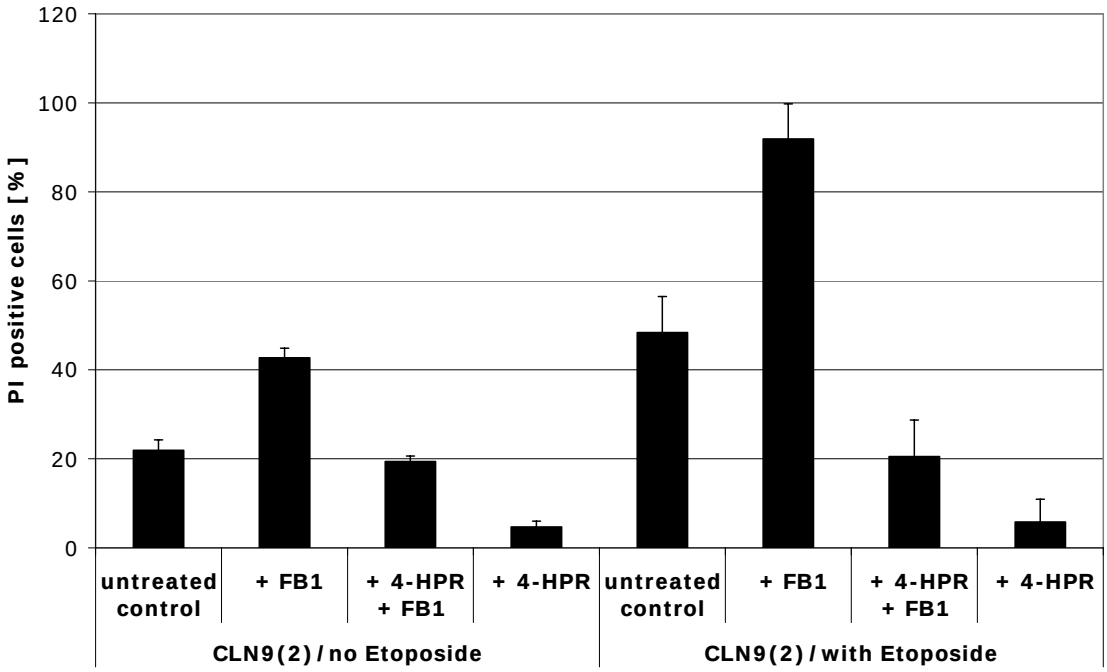
120
100
80
60
40
20
0
PI positive cells [%]
untreated control
+ FB1
+ 4-HPR + FB1
+ 4-HPR
untreated control
+ FB1
+ 4-HPR + FB1
+ 4-HPR
CLN9(2) / no Etoposide
CLN9(2) / with Etoposide

Fig. 6 C

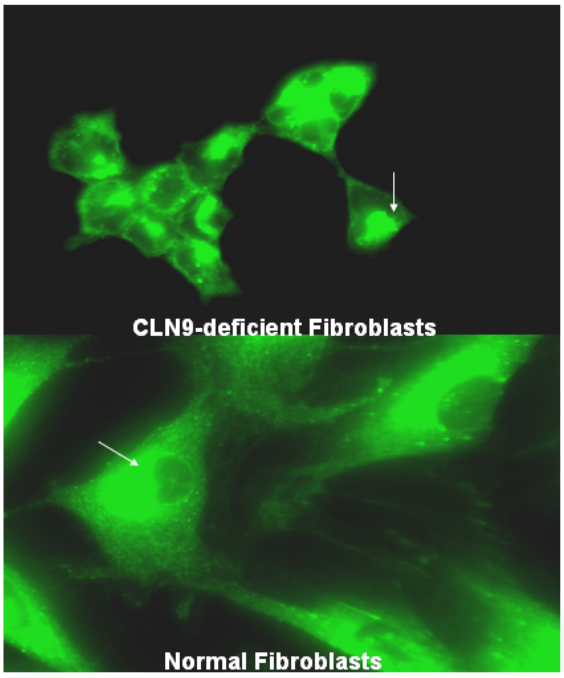
CLN9-deficient Fibroblasts
Normal Fibroblasts

Fig. 7

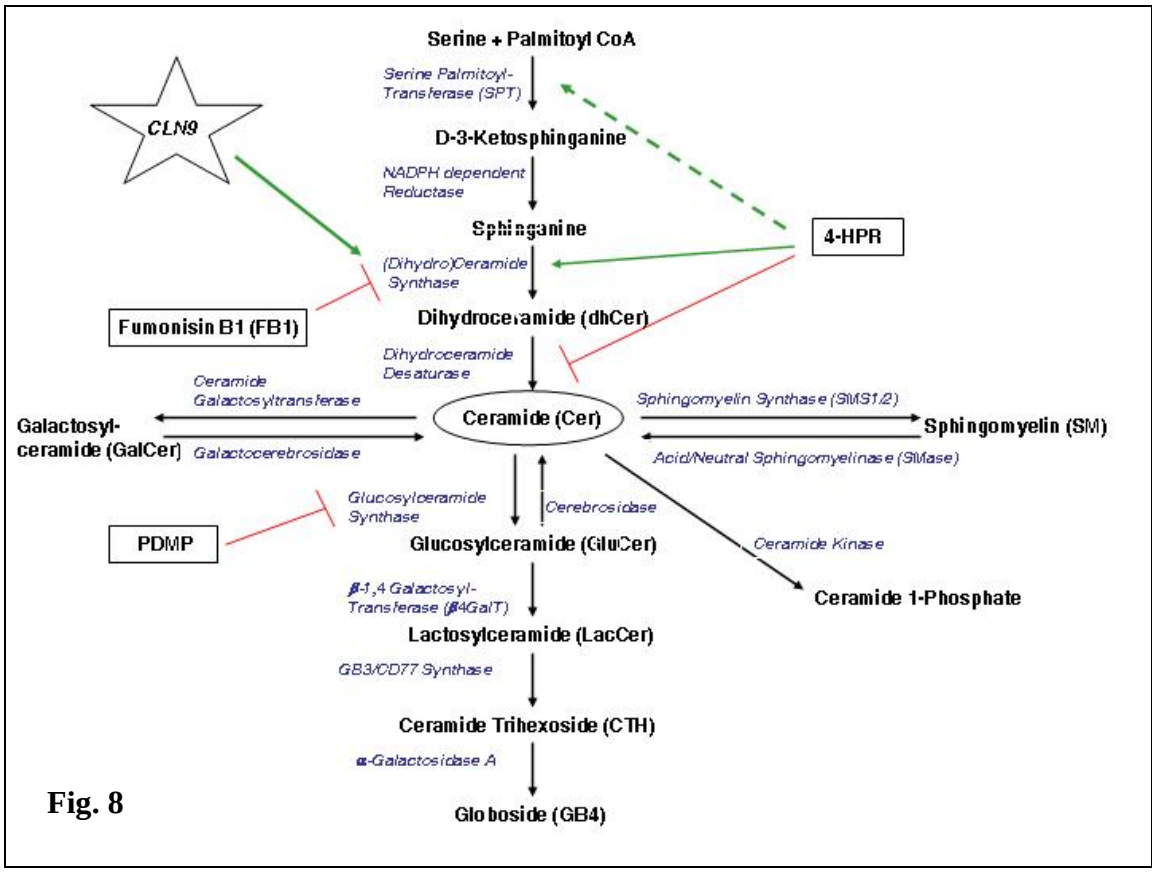
Serine + Palmitoyl CoA
Serine Palmitoyl-Transferase (SPT)
CLN9
D-3-Ketosphinganine
NADPH dependent Reductase
Sphinganine
4-HPR
(Dihydro)Ceramide Synthase
Fumonisin B1 (FB1)
Dihydroceramide (dhCer)
Dihydroceramide Desaturase
Ceramide Galactosyltransferase
Galactosyl-ceramide (GalCer)
Galactocerebrosidase
Ceramide (Cer)
Sphingomyelin Synthase (SMS1/2)
Sphingomyelin (SM)
Acid/Neutral Sphingomyelinase (SMase)
Glucosylceramide Synthase
Cerebrosidase
PDMP
Glucosylceramide (GluCer)
Ceramide Kinase
Ceramide 1-Phosphate
β-1,4 Galactosyl-Transferase (β4GalT)
Lactosylceramide (LacCer)
GB3/CD77 Synthase
Ceramide Trihexoside (CTH)
α-Galactosidase A
Globoside (GB4)

Fig. 8